Journal of Paleontology, 97(5), 2023, p. 971–989

0022-3360/23/1937-2337
doi: 10.1017/jpa.2023.13

JOURNAL OF PALEONTOLOGY
A PUBLICATION OF THE Paleontological SOCIETY

Micro-CT analysis of Katian radiolarians from the Malongulli Formation, New South Wales, Australia, and implications for skeletogenesis

Siyumini Perera and Jonathan C. Aitchison*

School of Earth and Environmental Sciences, The University of Queensland, St. Lucia, 4072, Queensland, Australia <p.perera@uq.edu.au>, <jona@uq.edu.au>

Abstract.—A diverse and well-preserved radiolarian assemblage from the Malongulli Formation, New South Wales, Australia, contains 13 species representing 10 genera and six families. One new genus, *Wiradjuri*, is introduced to accommodate pre-Devonian single-shelled entactiniid taxa, and one new species, *Secuicollacta malongulliensis*, is recorded together with some previously described forms. The microstructures of the "rotasphaerid structure/primary unit" and the "ectopic spicule" are investigated to validate their roles as fundamental units in the Secuicollactidae, together with comprehensive documentation of the previously enigmatic *Pseudorotasphaera* internal skeleton.

The results of this investigation suggest that, among all radiolarian genera that survived the Late Ordovician Mass Extinction event (LOME) and transitioned into the Silurian, *Secuicollacta*, *Haplotaeniatum*, and *Palaeoephippium* maintained stable body plans during the transition and were more successfully established. The selective advantages these lineages had during the LOME were most likely spontaneous outcomes of the mode of structural development involving sequential skeletogenesis and a tendency to evolve toward simpler body plans.

UUID: http://zoobank.org/264c026f-35af-4025-a4f7-de8f9a91f8b9

Introduction

Radiolarians are a major plankton group of the Paleozoic, capable of providing important insight into the evolution of heterotrophic plankton during their Ordovician diversification. Analysis of paleobiodiversity dynamics relies on documentation of chronostratigraphically well-constrained radiolarian assemblages (e.g., Danelian and Monnet, 2021).

Radiolarians from the Upper Ordovician Katian Stage were first reported from the Hanson Creek Formation in Nevada (Dunham and Murphy, 1976) and later revisited by Renz (1990). On the basis of conodonts from layers immediately above the radiolarian-bearing concretionary horizon, the assemblage represents the Ordovician Ka2 (mid-Katian) interval (Trotter and Webby, 1994). The Malongulli Formation of New South Wales, Australia, correlates with Ka2–Ka4 and was investigated for radiolarians by both Webby and Blom (1986) and Noble and Webby (2009). Several other nearby localities in the Lachlan Fold Belt possibly represent correlative Upper Ordovician horizons, albeit in different sedimentary facies (Goto and Ishiga, 1991; Goto et al., 1992). Apart from these Laurentian and Gondwanan sites, assemblages discovered from the Zhaolaoyu Formation in North China (Song et al., 2000) and the Wufeng Formation in South China (Wang and Zhang, 2011; Zhang et al., 2018) further broaden knowledge of the paleogeographic extent of Katian radiolarians. Obut (2022) recently reported Upper Ordovician radiolarians from deep shelf environments of the Siberian paleocontinent. This upper Katian to lower Hirnantian radiolarian assemblage from the western Gorny Altai region apparently shares several species with Katian assemblages previously recorded from New South Wales, Australia, and Nevada, USA, but awaits further detailed documentation.

The majority of known Katian faunas exhibit excellent to moderate preservation, but despite their significant position in the evolutionary history of early radiolarians, the systematics of several faunas remains vague (Aitchison et al., 2017a). This study investigates the diversity of a well-preserved and stratigraphically well-constrained Katian fauna of the Malongulli Formation in Australia with a focus on the microskeletons of *Secuicollacta* Nazarov and Ormiston (1984), *Palaeoephippium* Goodbody (1986) and *Haplotaeniatum* Nazarov and Ormiston (1987). These cosmopolitan genera were abundant at that time and evolved into major lineages that persisted across the Late Ordovician Mass Extinction (LOME).

The Angullong sampling site as described by Noble and Webby (2009) was chosen to facilitate recovery of well-preserved radiolarians for examination by micro-CT. This evolving methodology provides detailed three-dimensional (3D) imagery necessary to explore their skeletal signatures and undertake structural analysis, particularly, in the case of this investigation, of features in forms that survived the LOME. Systematics of several other taxa recovered from the assemblage that have

*Corresponding author.

been reported elsewhere are also revised. Both a new genus and new species are documented and added to knowledge of Katian radiolarian diversity (Aitchison et al., 2017b).

Geological setting

Locality information.—The Angullong section in the Malongulli Formation (33°34′57.58″S, 148°52′54.06″E), from which the studied sample SEES/210512-AB was collected, is an ~4 m thick outcrop. Exposure occurs on the northwest bank of the Belubula River on the Angullong farm property, ~15 km east of Canowindra, a township approximately 150 km west of Sydney, New South Wales, Australia (Fig. 1). The section consists of calcareous siltstone layers in which sponge spicules and radiolarian "ghosts" are visible. The Malongulli Formation (Stevens, 1952; Webby and Packham, 1982) crops out in the Cliefden Caves area and is part of the Cabonne Group within the Molong Volcanic Belt (MVB). This is one of the four structural belts in the Macquarie Arc in the eastern subprovince of the Lachlan Orogen (Glen et al., 1998, 2012). The formation is composed of calcareous siltstones, shales, spiculitic layers, tuffs, and limestone breccias (Stevens, 1952) hosting a wide array of fossil faunal assemblages representative of deep-water facies. The unit is >380 m thick (Percival, 1976) and unconformably overlies the shallow-water Cliefden Caves Limestone Subgroup (Vandon, Belubula, and Fossil Hill limestones), which is correlated with the Australian lower Eastonian (Ea1–Ea2) Stage (Webby and Peckham, 1982; Zhen and Webby, 1995). It is conformably overlain by the Angullong Formation, a succession of volcaniclastic sediments and andesites that is of Australian lower Bolindian (Bo1–Bo3) Stage (Percival and Glen, 2007).

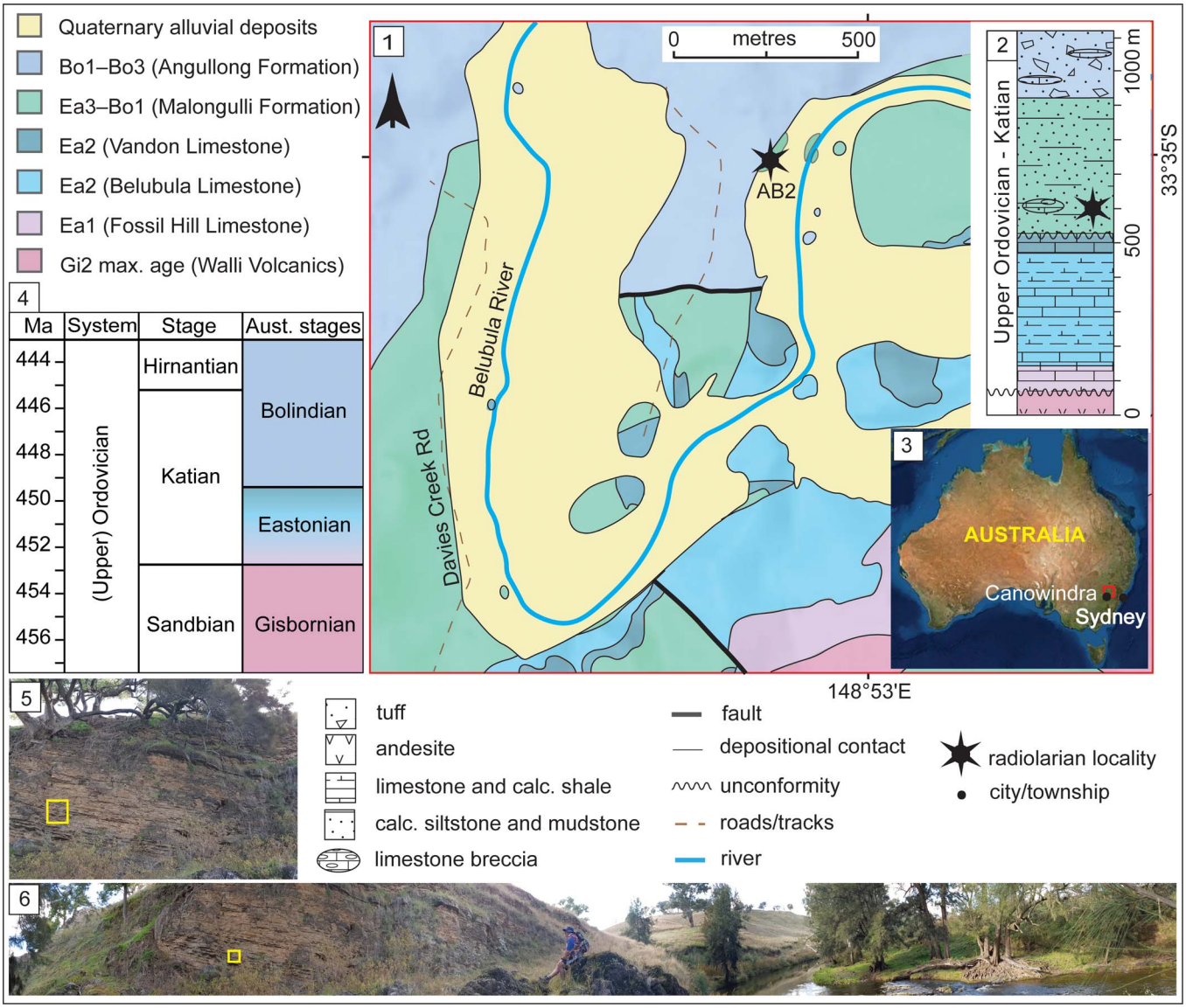

Figure 1. (**1**) Geological map of the Cliefden Caves study area (after Colquhoun et al., 2021 and references therein). (**2**) Generalized stratigraphic column for Ordovician strata in the Cliefden Caves area (modified from Rigby and Webby, 1988; Percival and Glen, 2007). (**3**) Overview map showing the location of study area. (**4**) Correlation of Australian to International stages. (**5**) Field photograph of the sampling site of SEES/210512-AB2. (**6**) Panoramic view field photograph of the Angullong sampling site on the Belubula River. Bo = Bolindian Stage; Ea = Eastonian Stage; Gi = Gisbornian Stage.

https://doi.org/10.1017/jpa.2023.13 Published online by Cambridge University Press

Deposition of the Malongulli Formation commenced when the sedimentary environment changed from benthic to pelagic, causing cessation of Cliefden Cave Limestone Subgroup deposition along the eastern flank of the MVB. Shallow-water sedimentation continued on the western flank of the MVB, resulting in occasional scouring and slumping from carbonate banks. This is a potential explanation for the erratic occurrence of limestone breccias in the Malongulli Formation (Webby and Peckham, 1982). More-detailed accounts of the geology, tectonics, and stratigraphy of the area are presented by Percival (1976), Webby and Peckham (1982), Rigby and Webby (1988), Webby (1992), Percival and Webby (1996), Glen et al. (1998), and Percival and Glen (2007).

Stratigraphic context.—Locally, the Malongulli Formation unconformably overlies the Vandon Limestone member of the Cliefden Caves Subgroup. The unit immediately below the Malongulli Formation a.k.a. "the Grey Unit" (Percival, 1976) is sparsely fossiliferous and lacks any age-diagnostic fossils. The base of the Malongulli Formation was first assigned to the *Dicranograptus clingani* Zone by Moors (1970), corresponding to the *D. kirki* Zone in Australasia (Cooper et al., 2004). This represents the Australian upper Eastonian (Ea3) Stage. Later, Percival (1976) discovered an assemblage including *Alulagraptus uncinatus* (Keble and Harris, 1925) and *Dicellograptus eastonensis* (Keble and Harris, 1925) reflecting the *Pleurograptus linearis* Zone of the British Ordovician stratigraphy, from a bed immediately below the overlying Angullong Formation. This extended the stratigraphic range of the Malongulli Formation to the lower (Bo1) Bolindian Australian Stage (Percival, 1976; Cooper et al., 2004; Percival et al., 2015). Conodonts reported from the Malongulli Formation by Trotter and Webby (1994) and Noble and Webby (2009) include a diverse assemblage of North American midcontinent and North Atlantic affinities correlating with the graptolite-based age assignments. In addition to these graptolite and conodont faunas, the Malongulli Formation has yielded one of the most diverse sponge assemblages recorded from the Upper Ordovician (Rigby and Webby, 1988; Webby and Trotter, 1993) and macrofossils including brachiopods, corals, stromatoporids, bryozoans, trilobites, and nautiloids (Percival, 1976; Stait et al., 1985; Percival et al., 2016).

Materials and methods

The fauna described herein comes from laminated calcareous siltstones approximately 1.5 m above the base of the section described by Noble and Webby (2009) at Angullong on the Belubula River. From the 10 samples collected, only one yielded sufficiently well-preserved radiolarians suitable for micro-CT scanning.

Approximately 5 cm^3 sized crushed pieces were immersed in a 15% acetic, 5% HCl solution for up to three weeks before the first wash. This was followed by wet sieving through the 355 µm and 63 µm sieves. The air-dried residue was then picked for radiolarians under a Leica M80 light microscope. Individual specimens were imaged using a desktop Hitachi TM3030 SEM before micro-CT scanning. The latter step was undertaken for only a few targeted radiolarian species requiring detailed systematic investigation.

Specimens of *Pseudorotasphaera* sp., *Secuicollacta malongulliensis* n. sp., *Wiradjuri subulate* Webby and Blom, 1986, *Palaeoephippium octaramosum* Renz, 1990, *Haplotaeniatum fenestratum* Goto, Umeda and Ishiga, 1992, *Haplotaeniatum prolatum* Noble and Webby, 2009, and *Haplotaeniatum spongium* (Renz, 1990) were scanned using a Zeiss Xradia Versa XRM-500 high-resolution micro-CT scanner at the Julius Kruttschnitt Mineral Research Centre, The University of Queensland. Specimens were mounted on 4 mm^2 squares cut from a few standard double-sided conductive adhesive carbon tabs, arranged along a line on a SEM specimen stub (Ø: 12.5 mm, pin length: 6 mm). X, Y, and Z coordinates of each specimen on the stub were determined by a preliminary scan carried out at a lower resolution of 3 µm to locate the specimens during the scan. Micro-CT data acquisition, artifact reduction, and analysis followed the method described by Kachovich et al. (2019) and Sheng et al. (2020) except for substitution of Norland Optical Adhesive 61 (NOA61) and acrylonitrile butadiene styrene (ABS) mounts with carbon tabs on SEM stubs. This replacement enhances the efficiency of the analysis and the accuracy of the 3D model generated by Avizo 9.7 (2020.2 version) volume-rendering software by reducing the number of lower-density constituents (ABS mount and NOA61 glue) that need to be digitally removed from the dataset during the manual segmentation.

Repositories and institutional abbreviations.—Specimens observed in this study are housed in the micropaleontology collection of the School of Earth and Environmental Sciences, The University of Queensland, Australia (SEES-UQ). SEES/210512 refers to the collection number, while AB2 is the sample number. The last three characters (SEES/210512-AB2-YYY) correspond to the species identification number. Other repositories mentioned herein include the Department of Geology, Faculty of Science, Shimane University (DGSU PR), Australian Museum (AM), Federal Fund of core material, paleontological, lithological, and oil collections of the oil-and-gas provinces of Russia (FF-P001), Paleontological Collections, Department of Geology, University of Alberta, Canada (UA), Institute of Geology, Beijing (BGIN), and Geological Institute, Moscow (GIN).

Results

Sample SEES/210513/AB2 yielded a diverse, well-preserved radiolarian assemblage with 13 radiolarian species representing 10 genera. Faunal composition along with relevant taxonomic assignments and their specimen abundance are presented in Table 1. The assemblage is dominated by spumellarians, with *Kalimnasphaera maculosa* Webby and Blom, 1986 being the most abundant taxon. The rest of the assemblage constitutes subordinate populations of entactinarians, archaeospicularians, and albaillellarians. One new genus, *Wiradjuri*, together with a new species, *Secuicollacta malongulliensis*, are introduced. Although sample SEES/210513/AB2 did not yield any graptolites or conodonts during the present study, the age of the

https://doi.org/10.1017/jpa.2023.13 Published online by Cambridge University Press

Table 1. List of radiolarians recovered from the Angullong/Belubula sampling site in the Malongulli Formation, New South Wales, Australia, during this investigation, indicating relative abundances of different taxa and faunal diversity. Calculations of shell dimensions are based on at least five specimens when available. If species count is less than five, all specimens were measured.

Order	Family	Taxa	Sample AB2
Albaillellaria	Ceratoikiscidae	*Protoceratoikiscum crossingi* Noble and Webby, 2009	1
Archaeospicularia	Secuicollactidae	*Pseudorotasphaera* sp.	1
		Secuicollacta malongulliensis n. sp.	16
		Secuicollacta stelligera Renz, 1990	4
Entactinaria	Entactiniidae	*Wiradjuri subulata* (Webby and Blom, 1986)	>50
	Palaeoscenidiidae	*Palaeoephippium octaramosum* Renz, 1990	>50
		Palaeopyramidium sp. A	1
		Procyrtis rustii Li, 1995	1
Spumellaria	Haplotaeniatidae	*Haplotaeniatum fenestratum* Goto, Umeda, and Ishiga, 1992	~10
		Haplotaeniatum prolatum Noble and Webby, 2009	~10
		Haplotaeniatum spongium (Renz, 1990)	>25
	Inaniguttidae	*Inanigutta complanata* (Nazarov, 1975)	~20
		Kalimnasphaera maculosa Webby and Blom, 1986	>75

Angullong/Belubula River Section in the Malongulli Formation has been assigned by Trotter and Webby (1994) and Noble and Webby (2009) to the lower half of the *Oulodus velicuspis* (conodont) Biozone of the North American midcontinent, which correlates to the international Ka2–3 stage slices (Goldman et al., 2020).

Discussion

Katian radiolarian diversity.—Hitherto, Katian radiolarian assemblages found around the globe demonstrated a relatively low species diversity compared with Early and Middle Ordovician radiolarian assemblages reported elsewhere. The dominant forms such as *Kalimnasphaera*, *Wiradjuri*, and *Secuicollacta* that are abundant in Katian assemblages are cosmopolitan and can be found consistently in all encounters despite being situated in separate paleogeographic regions. The few taxa that appear to be restricted within a region are not necessarily endemic but potentially result from misidentification, taphonomic biases, habitat (deep-water/shallow-water species), and a tendency to focus on new species in publications. The complete list of Katian radiolarians identified to date (Table 2) indicates that Australian assemblages have the richest diversity (>70% of total number of species). This is likely a result of the density of sample sites compared with other regions. To understand the true diversity distribution across paleogeographic regions, more studies targeting the Katian are encouraged.

Implications of skeletogenesis.—As the interval that immediately preceded the LOME, the Katian is significant and holds information crucial for understanding causative abiotic

Table 2. Katian radiolarian diversity reported from various paleogeographic regions globally.

Order	Family	Species	Australia[1]	China[2]	United States[3]	Russia[4]
Albaillellaria	Ceratoikiscidae	*Etymalbaillella yennienii* Li, 1995	✓			
		Protoceratoikiscum crossingi Noble and Webby, 2009	✓✓			
		Protoceratoikiscum chinocrystallum Goto, Umeda, and Ishiga, 1992	✓		✓	✓
		Protoceratoikiscum clarksoni Danelian and Floyd, 2001				✓
		Procyrtis rustii Li, 1995	✓			
Entactinaria	Entactiniidae	*Wiradjuri dunhilli* (Noble and Webby, 2009)	✓			
		Wiradjuri subulata (Webby and Blom, 1986)	✓✓		✓	✓
	Palaeoscenidiidae	*Palaeoephippium imbifurcus* (Renz, 1990)			✓	
		Palaeoephippium octaramosum Renz, 1990	✓✓		✓	
		Palaeopyramidium sp. A	✓			
Spumellaria	Haplotaeniatidae	*Haplotaeniatum fenestratum* Goto, Umeda, and Ishiga, 1992	✓			
		Haplotaeniatum ovatum Noble and Webby, 2009	✓			
		Haplotaeniatum prolatum Noble and Webby, 2009	✓✓			
		Haplotaeniatum spongium (Renz, 1990)	✓✓		✓	
	Inaniguttidae	*Inanigutta complanata* (Nazarov, 1975)	✓✓			✓
		Inanigutta jiangsuensis Wang in Wang and Zhang, 2011		✓		
		Inanigutta webbyi Wang in Wang and Zhang, 2011		✓		
		Kalimnasphaera maculosa Webby and Blom, 1986	✓✓✓		✓	✓
Archaeospicularia	Secuicollactidae	*Pseudorotasphaera* sp.	✓			
		Secuicollacta cassa (Nazarov and Ormiston, 1984)				✓
		Secuicollacta malongulliensis n. sp.	✓			
		Secuicollacta minuta Goto, Umeda, and Ishiga, 1992	✓			
		Secuicollacta ornata Goto, Umeda, and Ishiga, 1992	✓✓		✓	✓
		Secuicollacta sceptri Macdonald, 1998				✓
		Secuicollacta silex Goto, Umeda, and Ishiga, 1992	✓			✓
		Secuicollacta stelligera Renz, 1990	✓		✓	

[1]Malongulli Formation, New South Wales (Goto et al., 1992; Noble and Webby, 2009; this paper)
[2]Wufeng Formation, Jiangsu and Hubei (Wang and Zhang, 2011; Zhang et al., 2018)
[3]Hanson Creek Formation, Eureka County, Nevada (Dunham and Murphy, 1976; Renz, 1990)
[4]Tekhten Formation, NW Gorny Altai, West Siberia (Obut, 2022)

https://doi.org/10.1017/jpa.2023.13 Published online by Cambridge University Press

triggers leading up to this catastrophic event that caused 85% of marine species (Jablonski, 1991; Sheehan, 2001) to be extinct. As radiolarian studies have not yet been adequately extended toward the Hirnantian, the mid-Katian (Ka2–3 stage slices) radiolarian fauna documented herein may hold clues to structural adaptations that ultimately proved either advantageous or disadvantageous for survival during the times of increasing ecological stress.

Among several genera that crossed into the Silurian, *Secuicollacta*, *Haplotaeniatum*, and *Palaeoephippium* were more successful in establishing themselves in the early Silurian oceans. Although some morphological modifications occurred during speciation, the primary body plan of these genera remained constant during the transition. *Plussatispila* MacDonald (2006) has a single known occurrence in the Darriwilian (Kachovich and Aitchison, 2020) before its early Silurian acme and has not been recovered from investigated Katian localities. It is interesting to consider whether any specific structural features of *Secuicollacta*, *Haplotaeniatum*, and *Palaeoephippium* facilitated their smooth transition through times of environmental change.

Segmentation of the micro-CT model for *Secuicollacta malongulliensis* n. sp. provides some insights to skeletogenesis of the primitive secuicollactids. Considering the configuration of skeletal elements, the spicule evidently performed as the initial skeleton when primary skeletogenesis began. This was followed by secondary skeletogenesis that happened via primary units directly fused to the spicule through primary rods. Formation of primary units that are not directly linked to the spicule then followed. Finally, secondary bars may have developed to bridge components of all primary units and spicules, forming a coherent meshwork combining all primary and secondary centers of skeletogenesis. Test sphericity may be a function of curvature of buttressed spicular rays as the spicule is the primary center from which other features formed. This pattern of sequential skeletogenesis may have been a key to surviving the Hirnantian mass extinction. In flourishing conditions, the number of primary units may not be restricted, but evidently a test can be completed and enclosed even if the spicule can generate only a minimum of one or two primary units (hypothetically), and this may be more optimal in ecologically taxing circumstances.

The tendency to develop a pylome, observed among several Upper Ordovician radiolarians such as *Kalimnasphaera maculosa*, *Haplotaeniatum prolatum*, and *H. spongium*, as a favorable adaptation is difficult to determine as kalimnasphaerids became extinct while haplotaeniatids have successful Silurian pylomate descendants such as *H. aperturatum* Noble et al. (1998) and *H. cathenatum* Nazarov and Ormiston (1993). However, as observed by Won et al. (2002), the pylome is not consistently present in all individuals among Silurian pylomate haplotaeniatids, implying that there could also have been another favorable adaptation in the skeletal structure that was advantageous for survival.

In contrast to the haplotaeniatids of the pre-Katian and post-LOME oceans, skeletal architectures of *H. prolatum*, *H. spongium*, and *H. ovatum* Noble and Webby, 2009 are different. Micro-CT reconstructions show that the labyrinth compactness of *H. spongium* is less than that of mid- to lowermost Upper Ordovician forms of this genus (Maletz and Bruton, 2008; Pouille et al., 2014; Kachovich and Aitchison, 2020; Perera et al., 2020; Perera and Aitchison, 2022). However, the original morphology seems to return by the early Silurian for a majority of species (Noble et al., 1998; Noble and Maletz, 2000; Won et al., 2002; Umeda and Suzuki, 2005; MacDonald, 2006; Tetard et al., 2014). It is worth considering whether the simpler body plan of Katian haplotaeniatids was advantageous during less-favorable environmental conditions.

As primitive members of the Palaeoscenidiidae, both *P. octaramosum* and *Palaeopyramidium* sp. A had a dense cover of spinules that reduced considerably by the Silurian although the spicular system remained the same. Therefore, the simple yet robust spicular system possibly could be a favorable adaptation that offered the lineage a better chance of survival.

Systematic paleontology

Phylum Radiozoa Cavalier-Smith, 1987
Class Polycystina Ehrenberg, 1838, sensu Riedel, 1967
Order Albaillellaria Deflandre, 1953, emend. Holdsworth, 1969
Family Ceratoikiscidae Holdsworth, 1969, sensu Holdsworth, 1977
Genus *Protoceratoikiscum* Goto, Umeda, and Ishiga, 1992

Type species.—*Protoceratoikiscum chinocrystallum* Goto, Umeda, and Ishiga, 1992 (pl. 17, fig. 1) from the Warbisco Shale, northwest of Taralga, New South Wales, Australia.

Protoceratoikiscum crossingi Noble and Webby, 2009
Figure 2.3

2009 *Protoceratoikiscum crossingi* Noble and Webby, p. 553, figs. 4.1–4.3.

Holotype.—Specimen (AM.F. 135539) from the Malongulli Formation, New South Wales, Australia (Noble and Webby, 2009, fig. 4.1).

Remarks.—A very rare species in the samples processed, from which only a fragment of a single specimen was recovered.

Order Archaeospicularia Dumitrica, Caridroit, and De Wever, 2000
Family Secuicollactidae Nazarov and Ormiston, 1984
Genus *Pseudorotasphaera* Noble, 1994

Type species.—*Pseudorotasphaera hispida* Noble, 1994 (pl. 3, fig. 5) from Payne Hills, Caballos Novaculite, Marathon Basin, west Texas, USA, by original designation.

Diagnosis.—Latticed, polygonal to spherical cortical shell and loosely latticed medullary shell joined through up to 10 primary beams of lower primary units that are directly connected with the base of upper primary units (UPUs). Four to six primary bars radiating from the bases of primary spines and primary beams. Fusion of lower primary units (LPUs) and upper primary units contributes, respectively, to form the cortical and medullary shell lattices incorporated with

https://doi.org/10.1017/jpa.2023.13 Published online by Cambridge University Press

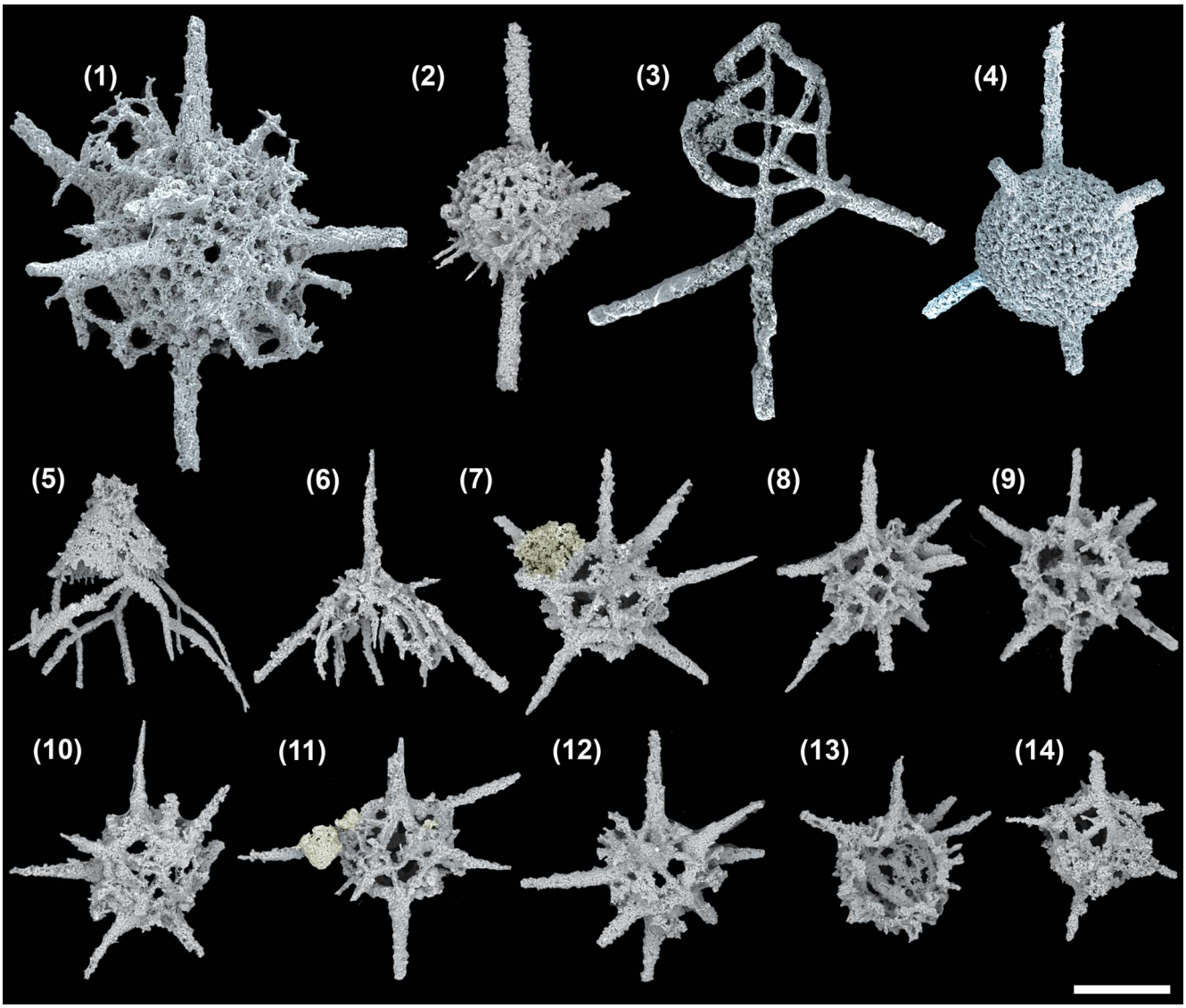

Figure 2. SEM images of radiolarians extracted from the Angullong/Belubula section, Malongulli Formation, New South Wales, Australia. (**1**) *Kalimnasphaera maculosa* SEES/210512-AB2-KM1; (**2**) *Wiradjuri subulata* SEES/210512-AB2-WS2; (**3**) *Protoceratoikiscum crossingi* SEES/210512-AB2-PC1; (**4**) *Inanigutta complanata* SEES/210512-AB2-IC1; (**5**) *Procyrtis rustii* SEES/210512-AB2-PR1; (**6**) *Palaeopyramidium* sp. A SEES/210512-AB2-PA1; (**7–12**) *Secuicollacta malongulliensis* n. sp. SEES/210512-SM2–SM7 (**13, 14**) *Secuicollacta stelligera* SEES/210512-AB2-SS1, -SS2. Scale bar = 100 µm. A faint yellow color is added to differentiate siliceous material adhering to, but not part of, specimens shown in (**7**) and (**11**).

secondary bars. Medullary shell, with or without secondary beams. Rod-like or grooved primary spines and angular to subcircular pore frames. Emended from Noble (1994).

Remarks.—The original diagnosis of Noble (1994) is broadened herein to include Upper Ordovician forms that possess nongrooved primary spines, more than seven in number that lack secondary beams compared with species described from the Silurian. The amendment also partially adapts the terminology used by MacDonald (1998) to describe *Rotasphaera*, using terminology appropriate for highlighting differences in morphological features compared with single-shelled secuicollactids.

Pseudorotasphaera sp.
Figure 3; Supplemental Data 1

Description.—The cortical shell is spherical (Ø, ~115 µm) and constructed with up to 10 UPUs that link with the primary beams of the LPUs of the centrally located medullary shell (Fig. 3.1, 3.2). LPUs of the medullary shell (Ø, ~60 µm) are constructed of four or five primary bars radiating from the bases of primary beams (Fig. 3.3). These primary bars are irregular in shape but fuse with one another to form the lattice of the medullary shell in association with secondary bars (Fig. 3.7). The diameter of a primary beam is consistent along its length and averages 10 µm. These thick bases of the primary beams impose a polygonal shape to the medullary shell. Primary beams grow up to 20 µm, similar to the distance between cortical and medullary shell. The top of these primary beams provides the base and is the center of the UPUs on the cortical shell (Fig. 3.5). A UPU constitutes a primary spine and five to six primary bars radiating from its base. Neighboring UPUs

https://doi.org/10.1017/jpa.2023.13 Published online by Cambridge University Press

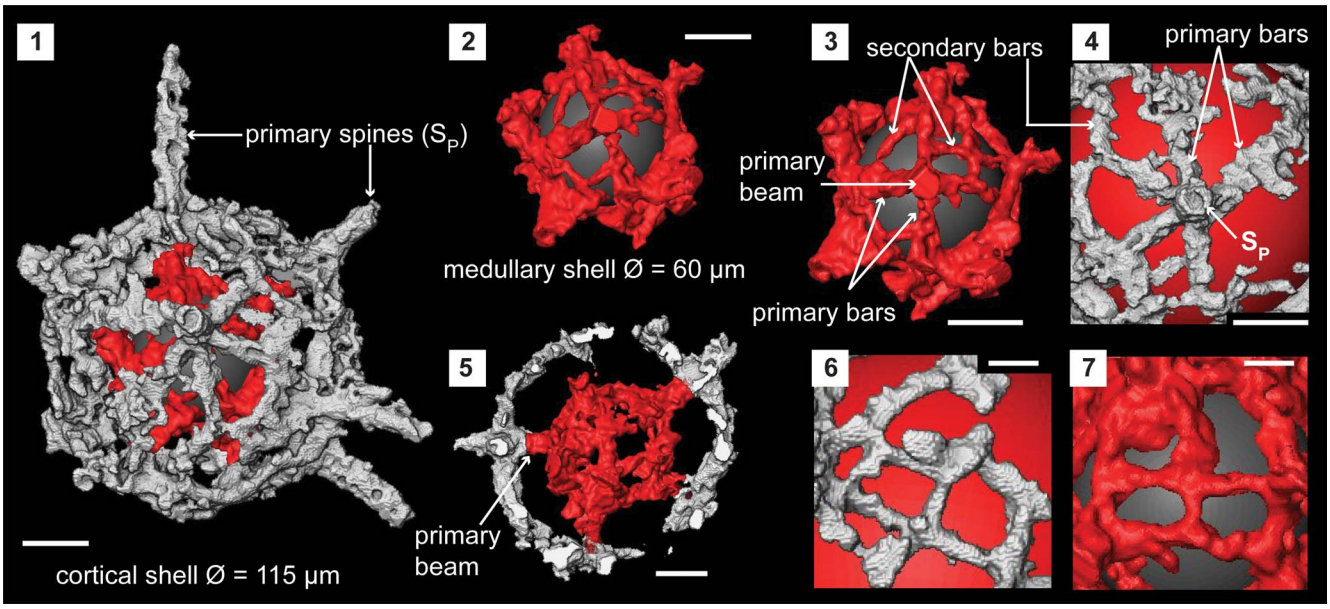

Figure 3. Structural details of *Pseudorotasphaera* sp. highlighted using a micro-CT model (SEES/210512-AB2-P1). (**1**) Complete specimen. (**2**) Medullary shell. (**3**) One lower primary unit (LPU) of the medullary shell comprising a primary beam, four primary bars, and secondary bars. (**4**) One upper primary unit (UPU) of the cortical shell comprises a primary spine, five primary bars, and secondary bars. (**5**) Cross section showing how a primary beam of an LPU connects to the base of a UPU. (**6**) Cortical shell lattice made by fusion of UPUs and secondary bars. (**7**) Medullary shell lattice made by fusion of LPUs and secondary bars. Gray and red spheres in (**1–4, 6, 7**) are inserted in the background to aid visualization. S_P = primary spines of UPU. (**1–5**) Scale bars = 25 µm; (**6, 7**) scale bars = 10 µm.

fuse with closely positioned primary bars and secondary bars that bridge to distant primary bars of other UPUs (Fig. 3.4). This coalescence creates polygonal-shaped pores that vary in size (Fig. 3.6). Primary spines are of circular cross section and taper distally to terminate with blunt ends. These extend up to 60 µm and have base diameters between 12 and 15 µm. No secondary beams on the medullary shell or secondary spines on the cortical shell.

Remarks.—Micro-CT observation of the skeleton of *Pseudorotasphaera* sp. confirms the presence of structures similar to primary units on the medullary shell. As the term "primary unit" generally signifies the special rotasphaerid structure that occurs exclusively on either the cortical or medullary shell of secuicollactids, the terminology in Figure 3 is applied to differentiate between the two types of primary units found on both medullary and cortical shells of *Pseudorotasphaera*. All LPUs of *Pseudorotasphaera* are relatively similar in size and equally prominent compared with *Diparvapila* MacDonald (1998), which has primary units of varying sizes (prominence) located on the medullary shell.

Pseudorotasphaera was initially placed in the Pseudorotasphaeridae (Noble, 1994), a family established to include taxa bearing two shells, cortical and medullary, made of primary units referred to as the "rotasphaerid structure." Won et al. (2002) suggested abandoning Pseudorotasphaeridae as a separate family as the number of shells could differ even at the genus level. In the unpublished thesis of MacDonald (2003), a classification based on the presence or absence of a spicule was recommended. Although it has been confirmed that both *Secuicollacta* and *Diparvapila* have ectopic spicules placed on their cortical and medullary shells, respectively, assignment of *Pseudorotasphaera* was undecided as available specimens were not sufficiently informative. Dumitrica et al. (2000) assumed the medullary shell of *Pseudorotasphaera* is spicular. Although *Secuicollacta* and *Diparvapila* have been thoroughly revised with additional multiple encounters, there are no subsequent reports of pseudorotasphaerids.

Pseudorotasphaera differs from *Secuicollacta* in having a medullary shell and lacking an ectopically placed spicule. The absence of a spicule is related to any preservational or ontogenetic bias such as that used as the rationale for synonymizing *Rotasphaera* with *Secuicollacta* (Noble and Maletz, 2000; Jones and Noble, 2006; Noble et al., 2017). Similar to *Pseudorotasphaera* sp., *Diparvapila* also has two shells, but the spicule is ectopically placed on top of the medullary shell along with a single primary unit at its opposite end. Even if the spicular rays of *Diparvapila* are mere primary units as argued by Won et al. (2002), another way to differentiate between *Pseudorotasphaera* and *Diparvapila* is that the latter has both a prominent and a small primary unit, whereas the former shows no difference except in the number of primary bars.

As only one specimen can be assigned to this Ordovician representative of *Pseudorotasphaera* at this stage, the extent of intraspecies variation remains uncertain. If more individuals are encountered, a new genus and species may be erected considering fundamental differences between Silurian and Ordovician pseudorotasphaerids such as a lack of secondary beams (beams between medullary and cortical shell that do not belong to an LPU) and the presence of spines with rod shapes rather than grooved forms. Differences in the number of spines may be a supplementary feature that varies at species level. It is clear that *Pseudorotasphaera* sp. is the oldest known ancestor of two-shelled secuicollactids, and Silurian pseudorotasphaerids and diparvapilids represent a single monophyletic group.

https://doi.org/10.1017/jpa.2023.13 Published online by Cambridge University Press

Genus *Secuicollacta* Nazarov and Ormiston, 1984 sensu MacDonald, 1998

Type species.—*Secuicollacta cassa* Nazarov and Ormiston, 1984 (pl. 4, fig. 5) from the Makyutov Complex, Tarangul River, Kosistek Village, southern Urals, Kazakhstan, by original designation.

Remarks.—Terminology used to describe Ordovician secuicollactids in earlier literature (Webby and Blom, 1986; Renz, 1990; Goto and Ishiga, 1991; Goto et al., 1992) reflects unfamiliarity with their spicular nature. This is subsequently acknowledged and discussed in detail by MacDonald (1998). Classification based on the number of "primary spines" sensu Goto et al. (1992) or "spines" sensu Renz (1990) is ambiguous and may lead to misidentifications. As Upper Ordovician secuicollactids are the most primitive members of their lineage, spicules of some species may not be easily discernible unless analyzed in a 3D space. Therefore, based on the broadened understanding on the skeletal microstructure offered through micro-CT, it is recommended to use the updated criteria adapted herein for differentiation of early members. This may result in fewer species as more emphasis will be placed on intraspecies variation. However, it will likely also lead to more accurate recognition of phylogenetic affiliations.

Secuicollacta malongulliensis new species
Figures 2.7–2.12, 4; Supplemental Data 2

1986 Rotasphaerids, Webby and Blom, p. 154, fig. 4.9, 4.10.
2009 *Secuicollacta ornata*; Noble and Webby, p. 553, fig. 4.6.

Holotype.—Specimen no. SEES/210512-AB2-SM1 (Fig. 4, Supplemental Data 3) in the micropaleontology collection of SEES-UQ. Known from Katian limestone beds in the Malongulli Formation, New South Wales, Australia.

Paratypes.—Specimen nos. SEES/210512-AB2-SM2–SM7 (Fig. 2.7–2.12) in the micropaleontology collection of SEES-UQ. Known from Katian limestone beds in the Malongulli Formation, New South Wales, Australia.

Diagnosis.—An ectopically placed pentactine spicule fused with five to six primary units to form a hollow, single spherical shell. A coherent mesh fuses the spicule and primary

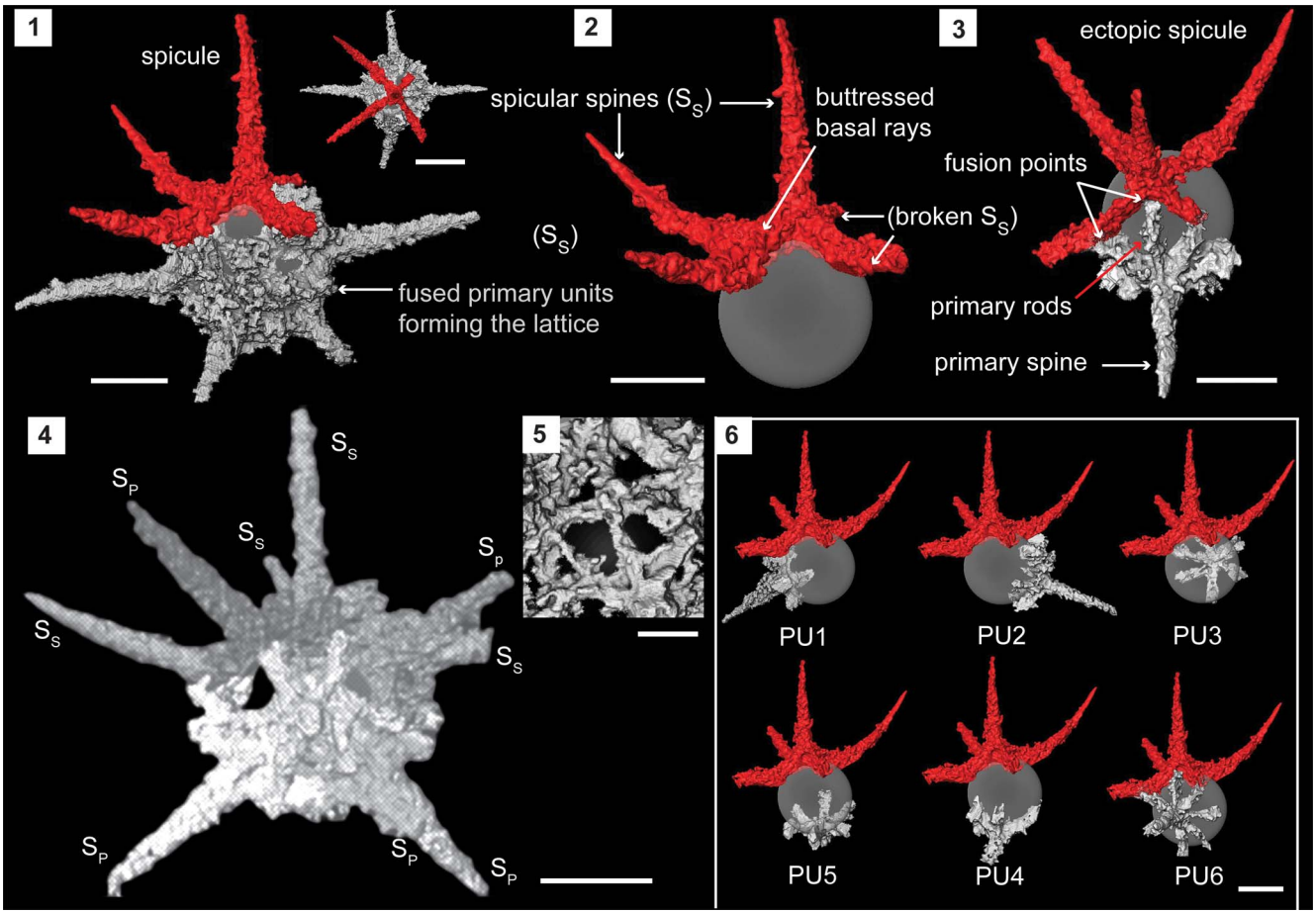

Figure 4. Structural details of *Secuicollacta malongulliensis* n. sp. highlighted using a micro-CT model (SEES/210512-AB2-SM1). (**1**) Complete specimen of *S. malongulliensis* n. sp. observed in two orientations. (**2**) Ectopically positioned initial spicule. (**3**) Primary unit highlighting its components and fusion with the spicule. (**4**) Example of an orientation that could obscure the spicule among the primary units. (**5**) Cortical shell lattice with polygonal pores. (**6**) Positions of all six primary units relative to the initial spicule. Gray sphere inserted to aid visualization. S_S = spicular spine; S_P = primary spine. (**1–4, 6**) Scale bars = 50 μm; (**5**) scale bar = 10 μm.

https://doi.org/10.1017/jpa.2023.13 Published online by Cambridge University Press

units, resulting in polygonal pores. Spicular and primary-spine lengths are slightly lesser or equal to the shell diameter. By-spines are rarely developed.

Occurrences.—Katian in Australia (Webby and Blom, 1986; Noble and Webby, 2009; this paper).

Description.—Micro-CT observations show the skeleton is constructed exclusively of a spicule, which includes the initial skeleton and several primary units. On the scanned specimen, the spicule demonstrates a fixed geometry where it comprises five rays positioned nearly perpendicularly to three adjacent spicular rays (Fig. 4.1). All five spicular rays are arranged on two planes where one ray occupies an apical position. The rest of the rays lie on a basal plane perpendicular to the first. All four basal spicular rays develop from the base of the apical spicular ray with rigid buttresses (Fig. 4.2). Beyond where the spicular rays extend from the perimeter of the spherical shell (represented by a hypothetical gray sphere in Fig. 4.2), they rise as independent spines (S_S) before inclining toward the apical spicular spine. The degree of inclination varies among specimens. A primary unit is composed of a primary spine (S_P) perpendicular to the primary rods that radiate from the base of the primary spine (Fig. 4.3). Individual specimens have five or six primary units (Fig. 4.5). The number of primary rods is generally between five and seven and may differ from unit to unit even within the same specimen (Fig. 4.5). Unlike spicular spines, primary spines are commonly straight (Fig. 4.4). Both spicular and primary spines taper distally while typically growing to within a few micrometers of the shell diameter. Spicular spines are usually longer than primary spines (S_S: 100 µm; S_P: 92 µm). Primary rods fuse with the neighboring primary rods of adjacent primary units or/and with neighboring spicular rays if present (Fig. 4.3). The coarse lattice developed among the primary units and the spicule initiates at multiple points of the skeletal elements and forms a coherent lattice with polygonal pores (Ø, 10–15 µm) (Fig. 4.5). The diameter of the outer shell ranges between 80 and 120 µm. The spherical shell wall is ~17 µm thick around spine bases and ~2 µm thinner elsewhere. By-spines are very rare and, if present, <5 µm long. The presence of by-spines is likely a random trait and not useful as in the characterization of Silurian secuicollactids.

Etymology.—Named after the Malongulli Formation from which the specimens were recovered.

Materials.—Sixteen specimens from the Malongulli Formation, New South Wales, Australia. Average measurements are based on six specimens.

Remarks.—Substantial secondary overgrowth of authigenic silica on examined specimens may have altered shell thicknesses and pore diameters by ±5 µm (Fig. 2.10, 2.12). Considering the new understanding of the microstructure, a revision of the diagnosis of all Ordovician secuicollactids is encouraged as, at the present state of knowledge, the nature of the spicule is hard to resolve. MacDonald (1998) suspected that specimens of *S. ornata* illustrated by Goto et al., 1992 have a three-rayed spicule although pentactines are the most common type of spicule found in secuicollactids. In respect to the much-discussed topic of whether secuicollactids have a true ectopic spicule or a special rotasphaerid structure (Furutani, 1990; Wakamatsu et al., 1990; Noble, 1994; MacDonald 1998; Dumitrica et al., 2000; Won et al., 2002; Jones and Noble, 2006), micro-CT observations support the first hypothesis as the spicule can be readily dissected from the rest of the rotasphaerid structures that are acknowledged herein as primary units following MacDonald (1998). The ortho slices (2D projections) show the point of radiation of the five rays although fusion between primary units and spicules makes segmentation challenging. Reexamination will be required to confirm whether all specimens reported from the Upper Ordovician (Webby and Blom, 1986; Renz, 1990; Goto et al., 1992; Noble and Webby, 2009) as secuicollactids have a spicule or not.

The number of primary units should not be a sole criterion for species differentiation as intraspecies variations likely fall within an admissible range. The number of spicular rays and their configuration appears to be relatively constant within any given species. The task of identifying the spicule from among the interconnected primary units is challenging and requires thorough observation (Fig. 4.4). If an initial spicule is prominent, differentiation among species on the basis of test dimensions is not recommended as ontogeny and environmental conditions likely result in intraspecific variation. Meshworks developed from fusion of skeletal elements during late stages of skeletogenesis are distinctive and can be used for characterization together with the spicule availability and their configuration.

Secuicollacta stelligera Renz, 1990
Figure 2.13, 2.14

1990 *Secuicollacta stelligera* Renz, p. 376, pl. 2, figs. 1, 4, 5.

Holotype.—Specimen (MR40 2A, V-8-0) from the Malongulli Formation, New South Wales, Australia (Renz, 1990, pl. 2, fig. 5).

Description.—Small secuicollactid constructed of an ectopically placed pentactine spicule and up to three primary units. Sphere (Ø, 90 µm) formed by coalescing straight primary and secondary bars in an angular meshwork. Short, tapering primary spines (~45 µm) are straight and slender compared with spicular rays that curve slightly toward the perpendicular spicule ray.

Remarks.—Although smaller individuals of *S. ornata* Goto, Umeda, and Ishiga (1992) and *S. malongulliensis* n. sp. may have shell diameters approaching 80 µm as with *S. stelligera*, the meshwork of *S. stelligera* is strongly angular, and it has larger pore spaces compared with other species in the genus. *S. stelligera* and *S. silex* Goto, Umeda, and Ishiga (1992) may have similar shell diameter, but the length of the primary spines of the latter is almost similar to its sphere diameter whereas spines of *S. stelligera* are only half of its shell diameter.

https://doi.org/10.1017/jpa.2023.13 Published online by Cambridge University Press

Order Entactinaria Kozur and Mostler, 1982
Family Entactiniidae Riedel, 1967, emend. Won, 1997
Genus *Wiradjuri* new genus

Type species.—*Wiradjuri subulata* Webby and Blom, 1986 (AM.F. 134752) from the Malongulli Formation, New South Wales, Australia (Webby and Blom, 1986, fig. 2.9, 2.10).

Diagnosis.—Spherical skeleton with one porous lattice shell, and rarely with members bearing an additional thick spongy layer connected to the lattice. Eccentric median microbar-centered six-rayed initial spicule (up to 11 µm) that continues as six rod-like primary spines with larger diameters.

Occurrence.—Katian from Australia (Webby and Blom, 1986; Goto et al., 1992; Noble, 2000; Noble and Webby, 2009; herein), United States (Renz, 1990), China? (Wang and Zhang, 2011; Zhang et al., 2018), and Russia (Obut, 2022).

Etymology.—Acknowledging the :Wiradjuri Nation," the group of First Nations people living in the central New South Wales region from which the type specimen was found.

Remarks.—*Wiradjuri* n. gen. is introduced in this study to include bar-centered, six-rayed, single-shelled entactiniids that are widespread among Katian radiolarian assemblages. Constituent species include *Wiradjuri subulata* (Webby and Blom, 1986) and *Wiradjuri dunhilli* (Noble and Webby, 2009). Webby and Blom (1986) introduced *W. subulate* as *Entactinia subulate*, and this usage was followed by Renz (1990) and Noble (2000). As *Entactinia* Foreman (1963) is a junior synonym of *Stigmosphaerostylus* Rüst, 1982 (Aitchison and Stratford, 1997; Noble et al., 2017) and these forms have rod-like rather than three-bladed spines, Noble and Webby (2009) reassigned them within *Borisella* Afanasieva (2000) along with *W. dunhilli*, another species with an extra spongy outer layer. However, both these Katian species differ significantly from the Devonian (upper Frasnian) type specimen, *Borisella maksimovae* Afanasieva, 2000. In contrast to the rod-like primary spines of *Wiradjuri*, *Borisella* has primary spines with "Y-shaped" basal cross sections similar to other entactiniids with bladed spines and a relatively short median microbar (<8.5 µm). Ordovician radiolarians that have been assigned to *Borisella* are abundant in Upper Ordovician strata of Australia (Webby and Blom, 1986; Noble and Webby, 2009; herein), the United States (Renz, 1990), and Russia (Obut, 2022). However, they have no obvious successors until considerably higher in the Upper Devonian. This prolonged stratigraphic hiatus of around 70 million years is not realistic, and reassignment of species that were previously known as *Borisella subulata* Noble and Webby, 2009 and *Borisella dunhilli* Noble and Webby, 2009 to the new genus *Wiradjuri* seems justified. The micro-CT observations reveal diagnostic morphological features associated with the type species, *Wiradjuri subulata*, that provide a basis for precise identification of *Wiradjuri* n. gen. in future encounters.

Inanigutta webbyi Wang in Wang and Zhang, 2011 and *Inanigutta jiangsuensis* Wang in Wang and Zhang, 2011 recovered from the upper Katian Wufeng Formation reportedly have a layer of spongy material on top of a latticed shell along with six rod-like primary spines. These could also potentially be members of *Wiradjuri* n. gen. and may be related to, or even synonymized with, *W. dunhilli*. However, the structure of their inner elements remains unclear at present.

Wiradjuri subulata (Webby and Blom, 1986)
Figures 2.2, 5; Supplemental Data 3

1986 *Entactinia subulata* Webby and Blom, p. 149, fig. 2.7–2.11.
1990 *Entactinia* sp. aff. *E. subulata*; Renz, p. 370, pl. 1, figs. 4, 6, 8, 10.
2000 *Entactinia* sp. aff. *E. subulata*; Noble, pl. 1, figs. 5, 6.
2009 *Borisella subulata*; Noble and Webby, p. 555, fig. 4.9.

Holotype.—Specimen (AM.F. 134752) from the Malongulli Formation, New South Wales, Australia (Webby and Blom, 1986, fig. 2.9, 2.10).

Description.—*Wiradjuri subulata* comprises a six-rayed median microbar-centered spicule, single thick latticed spherical shell, and six rod-like primary spines that are direct continuations of the six rays (Fig. 5.1, 5.2). In the initial skeleton, the spicule is eccentric and constructed of a median microbar (MB) of 11 µm in length. Three spicular rays (R_S) initiate from each end of the MBs and continue until they meet the lattice shell. Rays are about 5 µm in diameter and range from 20 to 50 µm long depending on the position of the spicule inside the shell (Fig. 5.4, 5.5). Configuration of the rays is not definitive, but most specimens have a ray from both ends of the MB developing in an apical and anti-apical direction. The remaining four rays are arranged nearly perpendicular and close to being in a single plane (Fig. 5.3). The hollow, thick-walled (10–15 µm), porous, latticed, spherical shell (~Ø, 125 µm) exhibits subspherical to subangular pores of varying sizes (10–15 µm) (Fig. 5.6). Upon surfacing, slender spicular rays convert to massive rod-like primary spines with a base diameter of ~25 µm and median diameter of 20 µm for the rest of their length (Fig. 5.3). These may develop straight or slightly curved and terminate with tapered ends that can be curved, bifurcated, or straight. Rare, thin by-spines up to 20 µm long may develop from pore frames (Figs. 2.2, 5.1).

Remarks.—*Wiradjuri subulata* exhibits a high degree of intraspecific variation, mainly in the shape of primary spines. Observed specimens do not exhibit spine torsion or bifurcation of their distal ends. As observation of the initial spicule is highly subject to taphonomy, *W. subulata* with straight spines may be confused with juveniles of *I. complanata* Nazarov and Ormiston (1984), which also have a very delicate internal structure.

Family Palaeoscenidiidae Riedel, 1967 emend. MacDonald, 2004
Genus *Palaeoephippium* Goodbody, 1986

https://doi.org/10.1017/jpa.2023.13 Published online by Cambridge University Press

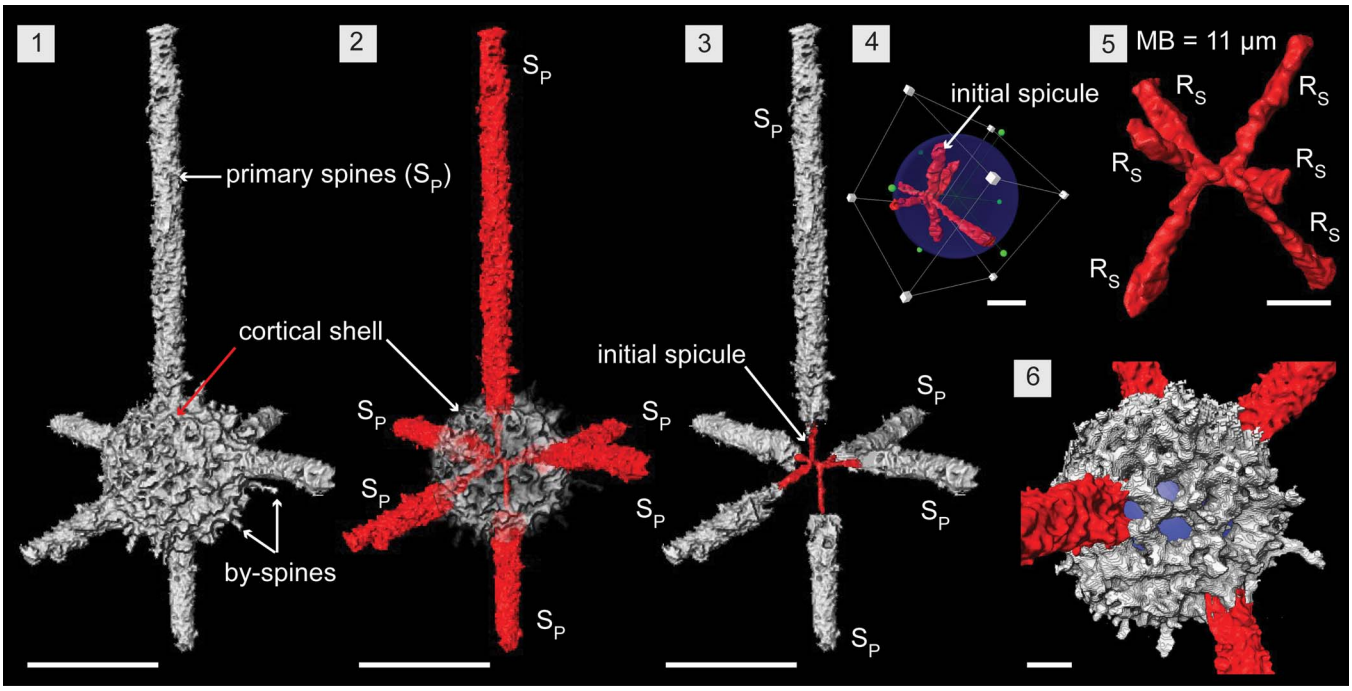

Figure 5. Structural details of *Wiradjuri subulata* highlighted using a micro-CT model (SEES/210512-AB2-WS1). (**1, 2**) Complete specimen of *W. subulata*. (**3**) Direct continuation of spicular rays as primary spines. (**4**) Eccentric position of the initial spicule within the shell. (**5**) Initial spicule highlighting components: median microbar and six spicular rays. (**6**) Shell lattice with subrounded pores. Blue spheres inserted to aid visualization in (**4, 6**). R_S = spicular ray; S_P = primary spine. (**1–3**) Scale bars = 100 µm; (**4–6**) scale bars = 25 µm.

Type species.—*Palaeoephippium bifurcum* Goodbody, 1986 (UA 7155) from the Cape Phillips Formation, Cornwallis Island, Canadian Arctic Archipelago by original designation.

Palaeoephippium octaramosum Renz, 1990
Figure 6; Supplemental Data 4

1986 Entactiniidae n. gen. n. sp. A; Webby and Blom, p. 150, fig. 2.1.
1986 aff. Entactiniidae n. gen. n. sp. A; Webby and Blom, p. 150, fig. 2.2.
1986 Entactiniidae n. gen. n. sp. B; Webby and Blom, p. 150, fig. 2.3–2.6.
1986 ?Entactiniidae n. gen. n. sp. B; Webby and Blom, p. 150, fig. 3.2.
1986 Entactiniidae (incerti generis) sp. 1; Webby and Blom, p. 151, fig. 3.3.
1990 *Palaeoephippium octaramosum* Renz, p. 370, pl. 3, figs. 1–3.
1990 *Palaeotripus sexabrachiatus*; Renz, p. 376, pl. 3, figs. 5, 7.
1990 *Palaeotrifidus ballator*; Renz, p. 374, pl. 3, figs. 4, 6, 8–10.
2009 *Palaeoephippium octaramosum*; Noble and Webby, p. 555, figs. 4.13–4.16, 6.12.

Holotype.—Specimen (MR40 2H, 0–39–0) from Hanson Creek Formation, Nevada, USA (Renz, 1990, pl. 3, fig. 3).

Description.—Skeleton constructed of a six-rayed initial spicule with an encircling girdle of spinules (Fig. 6.1, 6.2). Of the spicule's six rays, three radiate from each end of a short 30 µm long median bar. Two of the six rays are in an apical position and extend from either end of the median bar (Fig. 6.3, 6.5). These are rod-like, generally slightly curved, and taper toward their distal end with or without bifurcation. Length varies but is usually less than half that of the basal rays. There are three basal rays, two of which initiate from one end of the median bar, with the other starting from the opposite end (Fig. 6.4). All are rod-like and have a first bifurcation within the initial 30–35 µm from the median bar. Resultant branches continue to bifurcate at least once before terminating at pointed ends (Fig. 6.4). After the first bifurcation, multiple spinules develop off basal rays until all fuse densely to form an encircling girdle (Fig. 6.6). The sixth ray of the spicule could be in an intermediate position as in the scanned specimen (Fig. 6.3, 6.4) or in a basal position or an apical position. Regardless of the position of this sixth ray, it could bifurcate, although this is less common when it occupies an apical position.

Remarks.—The third apical ray reported in specimens of *Palaeotripus sexabrachiatus* Renz (1990) (presently a synonymy of *P. octaramosum*) is an example of the sixth spicular ray taking the apical position. Specimens figured and described as *P. octaramosum* by Renz (1990) reflect how this sixth ray can develop as a regular basal ray. Therefore, judging from all previous reports, the entire population of *P. octaramosum* demonstrates a high degree of intraspecies morphological variation driven primarily by the position of the sixth spicular ray. Systematics of the Palaeoscenidiidae are currently applied with an assumption that the existence of a similar geometric configuration is not necessarily indicative of

https://doi.org/10.1017/jpa.2023.13 Published online by Cambridge University Press

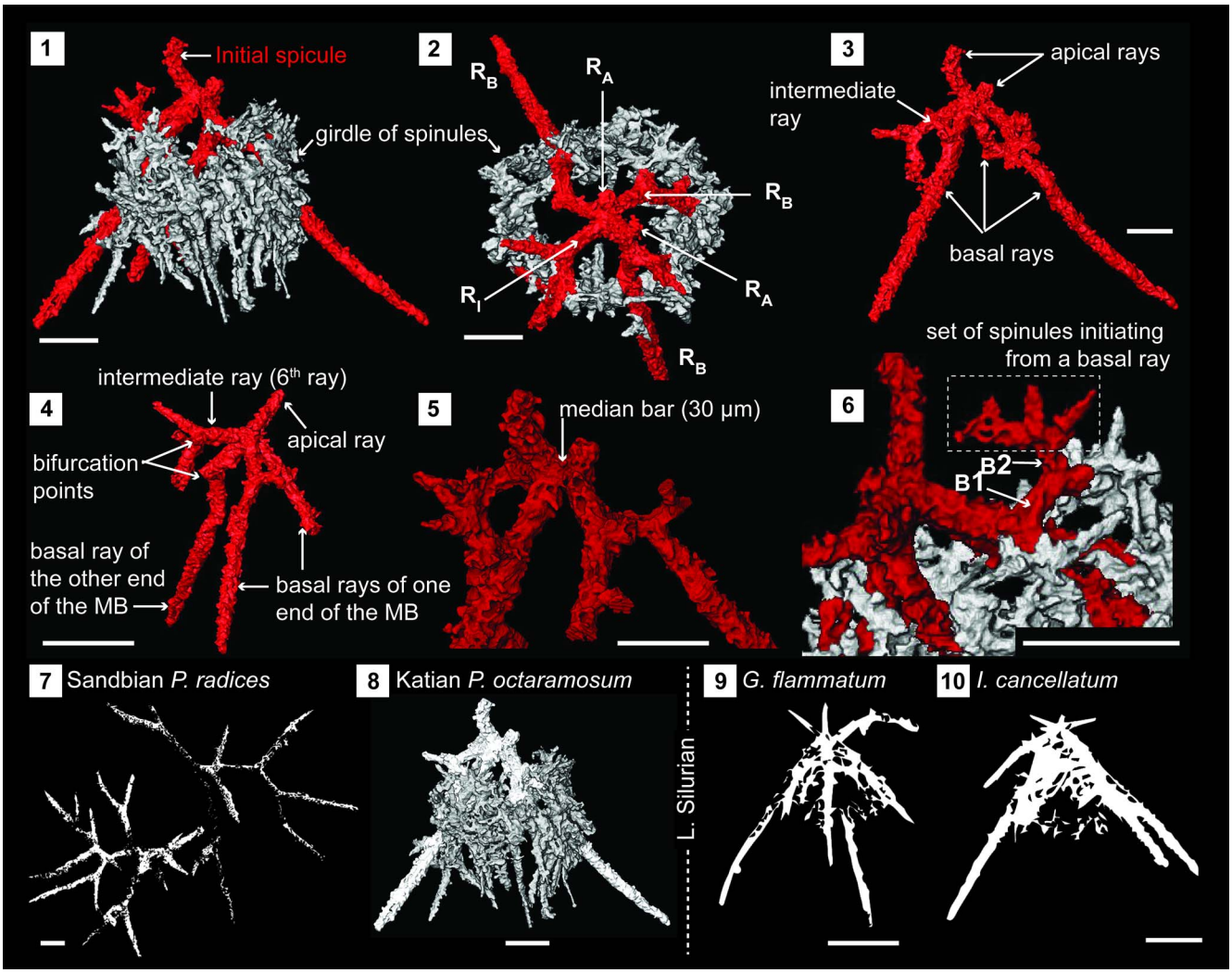

Figure 6. Structural details of palaeosceniids highlighted using a micro-CT model (SEES/210512-AB2-PO1). (**1, 2**) Complete specimen of *Palaeoephippium octaramosum* as seen in two orientations highlighting the skeletal elements. (**3, 4**) Initial spicule with specified ray arrangement and showing points of bifurcations. (**5**) Median bar. (**6**) Origination of spinules from first-order and second-order bifurcations. (**7–10**) Immediate phylogenetic affiliations indicating a possible evolutionary pathway from Sandbian to Llandovery forms. (**7**) Retraced from Perera and Aitchison (2022, fig. 12.9, 12.10). (**9, 10**) Retraced from MacDonald (2004, fig. 2.1, 2.9, respectively). R_A = apical ray; R_B = basal ray; R_I = intermediate ray; B_1 = first-order bifurcation; B_2 = second-order bifurcation. Scale bars = 50 µm.

a true phylogenetic relationship (MacDonald, 2004). Therefore, the key to understanding the generic affiliation of any given palaeoscenid is to properly differentiate the basic morphological features: the median bar/point, apical rays, basal rays, intermediate rays, and spinules. Differentiation among ray types is challenging under some circumstances. For an example, if intraspecies variations cause the intermediate ray to attain a basal position as in species of *Insolitignum* MacDonald, 1999, it promptly falls within the diagnosis of *Palaeoephippium*, resulting in potential confusion in generic assignment. The scanned specimen of *Palaeoephippium octaramosum* exhibits a similar scenario as one of the four basal rays takes an intermediate position. In addition, the specimen has two basal rays and an apical ray extending from one end of the median bar while the other end has a basal ray and an apical ray along with the ray in question, also satisfying the requirement for *Insolitignum*. This ray positioning is not uncommon as Noble and Webby (2009) mention that some specimens possess a ray in an intermediate position. Apart from the ray positioning, spinule development from basal rays to form a net-like tent is a characteristic of *Insolitignum* whereas *Palaeoephippium* is distinguished by ray branching. *Palaeoephippium octaramosum* strongly displays both these characteristic features and could be on an evolutionary pathway between the structurally simple Sandbian palaeoephipids that branch or bifurcate readily (e.g., *P. radices* Goodbody in Perera and Aitchison, 2022) and lower Silurian *Insolitignum* (e.g., *I. cancellatum* Goodbody, 1986) and *Goodbodium* Furutani, 1990 (e.g., *G. flammatum* Goodbody, 1986) types of genera with development of a prominent network of spinules (Fig. 6.7).

Genus *Palaeopyramidium* Goodbody, 1986

Type species.—*Palaeopyramidium spinosum* Goodbody, 1986 (UA 7136) from the Cape Phillips Formation, Cornwallis Island, Canadian Arctic Archipelago by original designation.

https://doi.org/10.1017/jpa.2023.13 Published online by Cambridge University Press

Palaeopyramidium sp. A
Figure 2.6

Description.—Point-centered skeleton composed of one apical ray and possibly four basal rays. Apical ray is pointed and oriented at 135° angle to the basal rays. Basal rays (~165 µm) are longer than the apical ray (~106 µm) and have blunt distal ends. Numerous spinules are present toward the proximal end of basal rays and visibly gather at the point center from which all rays diverge. Spinules are curved and arranged as a skirt around the basal rays and may extend up to two-thirds of the basal ray length. Maximum width of the basal hemisphere is 240 µm.

Remarks.—The single specimen encountered is not adequate for a species determination. Assignment at genus level is confident as, in addition to other diagnostic features, the angle maintained between the apical ray and basal rays is that of the type species *P. spinosum* Goodbody, 1986. The existence of a fourth basal ray is difficult to resolve among the spinules but can be assumed on the basis of the arrangement of the other three basal rays. A thick skirt of spinules is unique to this Ordovician form as all known Silurian and Devonian species of *Palaeopyramidium* demonstrate very weak to moderate development of spinules.

Genus *Procyrtis* Li, 1995

Type species.—*Procyrtis rustii* Li, 1995 (BGIN 920321) from the Baijingsi complex, Qilian Mountains, Qinghai Province, China, by original designation.

Procyrtis rustii Li, 1995
Figure 2.5

1995 *Procyrtis rustii* Li, p. 336, pl. 1, figs. 12, 17.

Holotype.—Specimen (BGIN 920321) from Baijingsi of Qinghai, China (Li, 1995, pl. 1, fig. 17).

Description.—Campanulate shell composed of a cephalis with an aperture and bifurcated rays extending from within. The upper cone-shaped segment or "cephalis" (vertical length = 95 µm) is composed of a shell open at the bottom with an aperture diameter of ~110 µm. The structure of the uppermost section of the cephalis is unclear due to poor preservation, and the existence of a horn (Li, 1995) is uncertain. Rays or "feet" of the specimen start bifurcating within their first 30 µm. They initiate as rods and taper after the first bifurcation to terminate with pointed ends. Rays may extend up to 150 µm long.

Remarks.—One specimen was recovered from the Angullong locality in the Malongulli Formation. The original type material (BGIN 920321) has been destroyed (L. Hui, personal communication, 2020). *Procyrtis qinglaii* Li, 1995 can be differentiated from *P. rustii* as the former has a short cephalis (maximum vertical height = 78 µm) with a smaller aperture diameter (51–78 µm). Assignment within the Palaeoscenidiidae by Noble et al. (2017) should be regarded as tentative until such time as a point center or a median bar can be confirmed within the cephalis from which the rays originate.

Order Spumellaria Ehrenberg, 1876
Family Haplotaeniatidae Won, Blodgett, and Nestor, 2002
Genus *Haplotaeniatum* Nazarov and Ormiston, 1993

Type species.—*Haplotaeniatum labyrintheum* Nazarov and Ormiston, 1993 (GIN 4679/33) from the Sakmarskaya Suite, Southern Urals, Russia, by original designation.

Haplotaeniatum fenestratum Goto, Umeda, and Ishiga, 1992
Figure 7; Supplemental Data 5

1992 *Haplotaeniatum fenestratum* Goto, Umeda, and Ishiga, p. 158, pl. 7, figs. 1–3.

Holotype.—Specimen (DGSU PR 1070) from the Malongulli Formation, northwest of Taralga, New South Wales, Australia (Goto et al., 1992, pl. 7, fig. 1).

Description.—A typical haplotaeniatid constructed of a proloculus and at least two whorls that are distinctly separated and without any primary or secondary spines. Slightly eccentric proloculus is not a complete spheroid yet exhibits a spherical outline with a maximum diameter of 38 µm in selected orientations (Fig. 7.1). The median whorl may reach double the size of the proloculus (60–82 µm) and is constructed of an irregularly porous, thick mesh different from the outer layers (Fig. 7.1, 7.3). Median whorl is closer to the proloculus than to the adjacent layer of the outer whorl as a space is maintained between them (Fig. 7.7). Coarse labyrinth of the outer whorl creates large pores with thin pore frames (3 µm) except at pore junctions. The majority of the subrounded pores lie within a diameter range of 15–30 µm with occasional small pores (Ø, 5–15 µm) (Fig. 7.2). Pore density of the outer whorls is very high compared with the median whorl. Whorls are interconnected at multiple points via small connecting bars (Fig. 7.5, 7.6). Clearly separated levels are not prominent in the outer whorl although the volume is much greater than that of the median whorl. The diameter of the spheroidal specimen ranges from 160 to 175 µm.

Remarks.—The terminology used by Goto et al. (1992) to describe their specimen is indicative of an approach where haplotaeniatids are considered to be spicular radiolarians. With the best understanding about the inner structure revealed through recent micro-CT observations, *Haplotaeniatum* is now considered to be a spumellarian. Less-distinct layering within the whorls is probably because *H. fenestratum* lacks spines, which define the levels of layering by developing apophyses along their lengths. Thus, the volume of the skeleton is developed with the help of multiple link points that extend as arches or bridges by initiating a new layer on top of their base layers. More points of linkage can be observed in the layers of *H. fenestratum* than on proloculi of other spinose haplotaeniatids.

Haplotaeniatum prolatum Noble and Webby, 2009
Figure 8; Supplemental Data 6

https://doi.org/10.1017/jpa.2023.13 Published online by Cambridge University Press

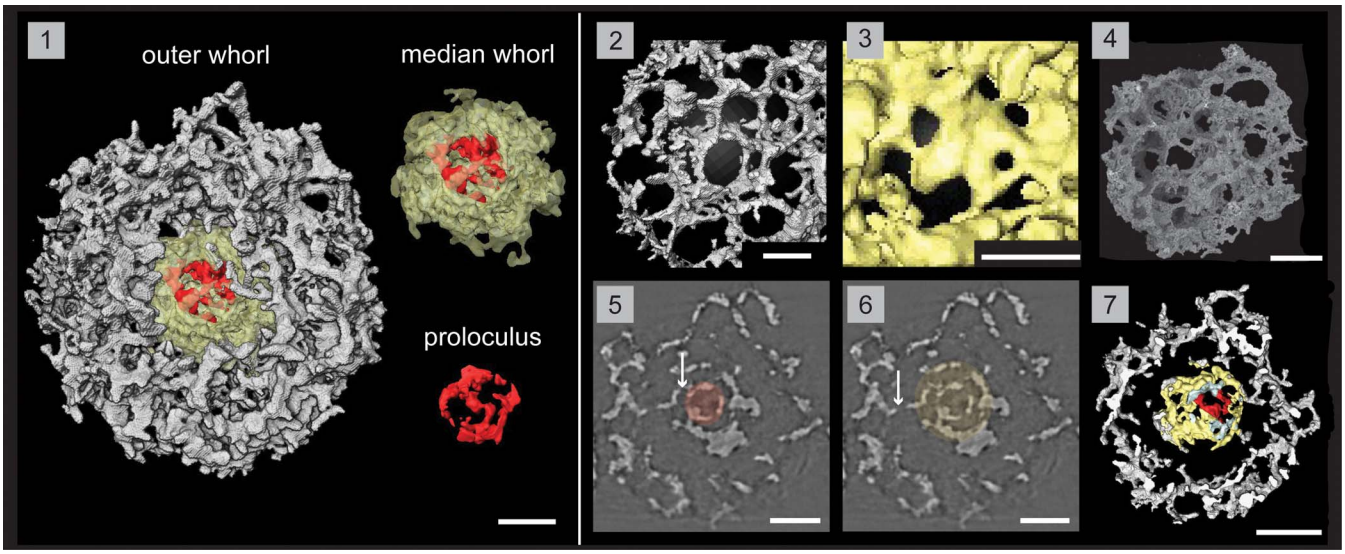

Figure 7. Structural details of *Haplotaeniatum fenestratum* highlighted using a micro-CT model (SEES/210512-AB2-HF1). (**1**) Complete specimen with separated whorls and proloculus. (**2**) Outer whorl labyrinth with larger pores and higher pore density. (**3**) Median whorl labyrinth with small pores. (**4**) SEM image of *H. fenestratum* (SEES/210512-AB2-HF2). (**5**) Original micro-CT image slice highlighting the proloculus. (**6**) Original micro-CT image slice highlighting the median whorl. (**7**) Cross section showing the space maintained between median and outer whorls. Arrows in (**5**) and (**6**) indicate connecting bars between whorls. (**1, 2**) Scale bars = 25 μm; (**3**) scale bar = 15 μm; (**4–7**) scale bars = 50 μm.

2009 *Haplotaeniatum prolatum* Noble and Webby, p. 557, figs. 5.4–5.6, 6.9, 6.10.

Holotype.—Specimen (AM.F.135567) from the Malongulli Formation, New South Wales, Australia (Noble and Webby, 2009, fig. 5.4).

Description.—The micro-CT reconstruction of *Haplotaeniatum prolatum* reveals it is constructed of a proloculus from which at least three primary spines (S_P) emanate and initiate a labyrinthine meshwork of whorls that randomly give rise to secondary spines (S_S). The proloculus (Ø, ~38 μm) is slightly eccentric and consists of bars that resemble a spheroid (Fig. 8.1). Three rod-like primary spines originate and radiate in a random configuration from the proloculus, which gradually tapers toward the distal end (Fig. 8.3). Multiple apophyses located at several levels of the primary spines produce a labyrinthine meshwork that engulfs the proloculus and approximately two-thirds of most of the spines. The diameter at the proximal end of the primary spines is about 5–10 μm, and observation of the delicate linkages with the proloculus is subject to preservation. Apart from these primary spines, the proloculus also develops a few short connecting bars to the nearest whorl of the meshwork (see arrow in Fig. 8.4). Apophyses toward the most proximal end of the primary spines collectively initiate the closest whorl of the meshwork and continue through each level of apophyses. A specimen may display whorls established via three to four discontinuous levels (Fig. 8.4). Secondary spines develop from random points on the whorls and become part of whorls by creating apophyses that densify the meshwork (Fig. 8.2). In general, both secondary and primary spines develop to a length of ~50 μm beyond the outer seam of the shell. The meshwork at one end commonly develops further toward the distal ends of two to four neighboring spines, incorporating them to create a pylome (Fig. 8.1, 8.2). This extension may appear as a "passage" in fully developed individuals. Subcircular to oval pores range in size (5–30 μm) and develop between thin (~4 μm), flat pore frames. Some pore frames appear as arches when pores are bigger and mostly located close to the seam of the shell. This 3D meshwork is approximately 170–200 μm at its widest.

Remarks.—The specimen used for the micro-CT observation is possibly a juvenile of *H. prolatum*. This inference is based on the incompletely developed passage that is still in the initial stages of incorporating neighboring spines.

As described by Goto et al. (1992), the diameter of the "most internal sphere" of *Haplotaeniatum spinatum* is 40 μm, and the number of spines (two to four) emanating from the most inner shell (probably the proloculus) can be matched with the specimen examined in this investigation. Other shell dimensions of *H. spinatum* support this, and it is recommended that it be removed from the *H. spongium* combination erected by Noble and Webby (2009) and placed within *H. prolatum*. Secondary spine development seems unrestrictive compared with that of primary spines, and the latter are fixed or at most vary within a very narrow range. Once both primary and secondary spines pass through the shell flanks, differentiation is not possible, and the number of spines finally emanating beyond the shell seam may be insufficient to distinguish *Haplotaeniatum* at species level. Development of the narrow passage associated with the pylome may be a characteristic trait of the *H. prolatum* although Won et al. (2002) considered the pylome of haplotaeniatids as an inconsistent taxonomic feature individualized to the specimen being observed.

Haplotaeniatum spongium (Renz, 1990)
Figure 9; Supplemental Data 7

https://doi.org/10.1017/jpa.2023.13 Published online by Cambridge University Press

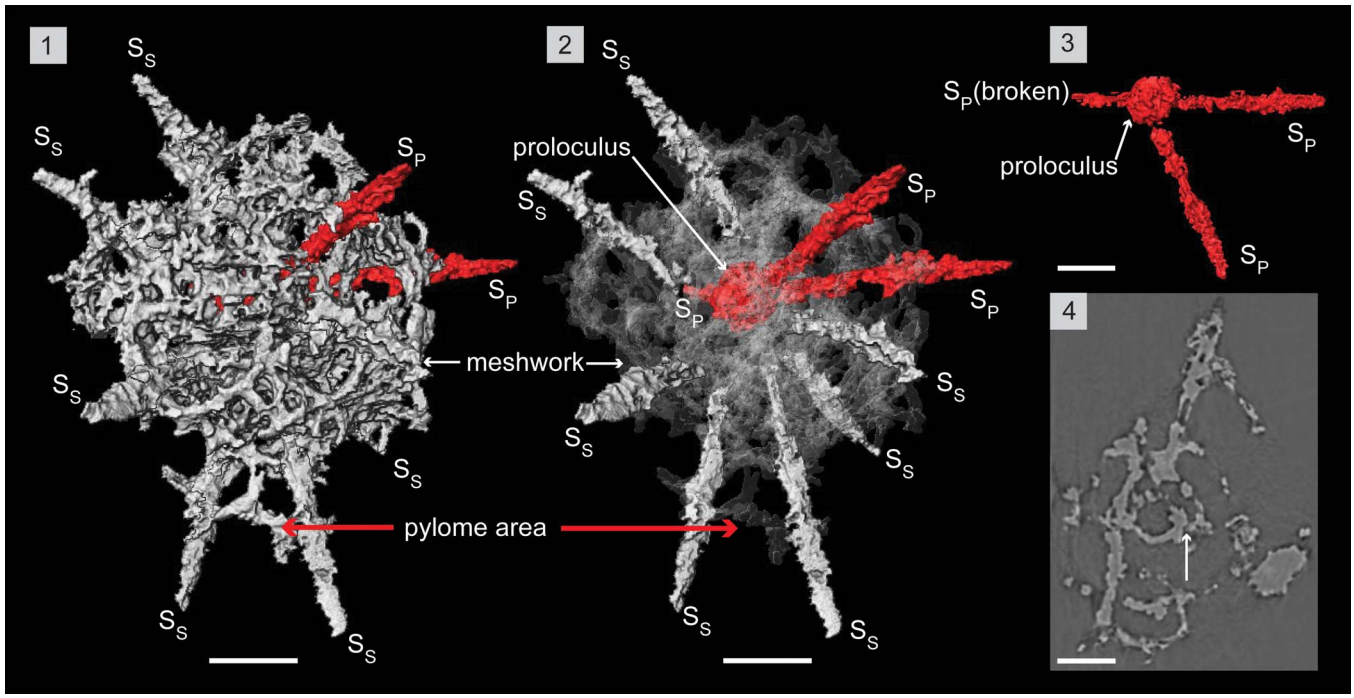

Figure 8. Structural details of *Haplotaeniatum prolatum* highlighted using a micro-CT model (SEES/210512-AB2-HP1). (**1**) Complete specimen. (**2**) *H. prolatum* highlighting its interior configuration of skeletal elements. (**3**) Primary spines emanating from the proloculus. (**4**) Original micro-CT image slice showing the whorls initiating as apophyses of spines. The arrow indicates a connecting bar between proloculus and the first whorl. S_P = primary spine; S_S = secondary spine. Scale bar = 50 µm.

1990 *Entactinia? spongia* Renz, p. 369, pl. 1, figs. 1–3.
1992 *Haplentactinia attenuata* Goto, Umeda, and Ishiga, p. 156, pl. 5, fig. 2, 3.

Holotype.—Specimen (MR40-1A, M-43-2) from the Malongulli Formation, New South Wales, Australia (Renz, 1990, pl. 1, fig. 2).

Diagnosis.—Haplotaeniatid with labyrinthine mesh consisting of more than two whorls around a small spheroidal proloculus. Six primary spines emanating from the proloculus and few to several secondary spines based at subsequent levels of the whorls that outgrow the shell flanks. Spine lengths are less than the shell diameter. No pylome. Emended from Renz (1990) and Noble and Webby (2009).

Description.—Haplotaeniatum spongium has a small proloculus from which six spines radiate together with a loose labyrinthine meshwork of more than two whorls that acts as the base for few to several secondary spines (Fig. 9.1, 9.2). The initial skeleton is the spheroidal proloculus (Ø, ~30 µm) located at the center of the shell. The proloculus gives rise to six delicate rod-like primary spines that are small at their bases but increase in diameter as they extend to at least half of their final length (~105 µm) before tapering toward their distal end. The configuration of primary spines is random and may vary among different specimens (Fig. 9.3). The apophyses of these primary spines develop further to define the whorls of the labyrinthine meshwork. When the labyrinth develops, secondary spines initiate from random locations on layers of the labyrinth, providing more apophyses to increase the mesh density of the shell. Secondary spine shapes are also similar to primary spines but shorter as they do not extend down to the proloculus. Primary and secondary spines may variably grow beyond the flanks of the shell. In general, both spines grow up to 45 µm beyond the flanks, but primary spines may grow up to 200 µm. The characteristics and the measurements of the labyrinthine meshwork (pore size, pore frames) are similar to the described *H. prolatum* although the labyrinth is comparatively less dense and has a faintly spiraliform nature in the labyrinthine arrangement under some orientations (Fig. 9.5, 9.6).

Remarks.—Ortho slices of the specimen SEES/210513/AB2/HS1 (Fig. 9.4) are similar to figure 6.11 of Noble and Webby (2009), highlighting the "moderately loose labyrinthine" character. The specimen in this investigation has 12 spines, among which six radiate directly from the proloculus, deviating from the species description of Noble and Webby (2009), who state that *H. spongium* has only six to eight spines. The six spines detected in specimens for this study could be a result of primary spines growing prominently compared with variably developed secondary spines. The number of secondary spines is not fixed and may be incorporated within the labyrinth, appearing simply as thick pore frames. Therefore, the diagnosis is broadened to include forms with more than eight spines.

Haplentactinia attenuata Goto et al. (1992) was described as having four to six primary spines and 8–15 by-spines that appear to be secondary spines. Although the shell diameter is less than the encountered specimens, its superficial appearance, length of spines, and pore sizes are closer,

https://doi.org/10.1017/jpa.2023.13 Published online by Cambridge University Press

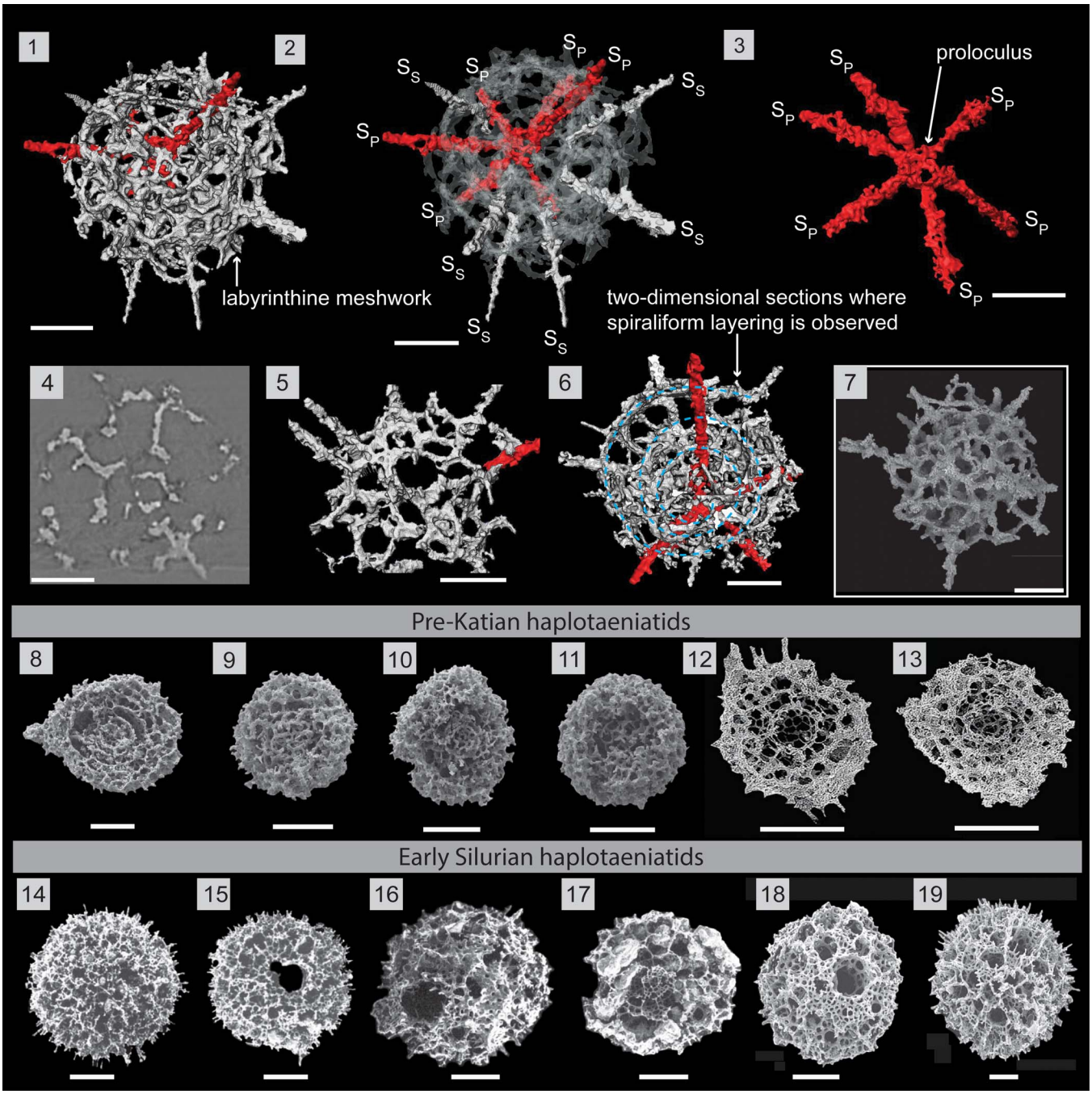

Figure 9. Structural details highlighted using a micro-CT model of *Haplotaeniatum spongium* (SEES/210512-AB2-HS1). (**1**) Complete specimen. (**2**) *H. spongium* indicating the interior configuration of skeletal elements. (**3**) Primary spines emanating from the proloculus. (**4**) Original micro-CT image slice showing the loose labyrinthine nature. (**5**) Outer whorl labyrinth with larger pores. (**6**) Specimen oriented to highlight two-dimensionality across a section where spiraliform layering (indicated by blue dashed lines) is observed. (**7**) SEM image of *H. spongium* (SEES/210512-AB2-HS2). (**8–13**) Pre-Katian haplotaeniatids. SEM images: (**8–11**) Pouille et al. (2014); (**12, 13**) Kachovich and Aitchison (2020). (**14–19**) Early Silurian haplotaeniatids. SEM images: (**14, 15**) Umeda and Suzuki (2005); (**16, 17**) Noble and Maletz (2000); (**18, 19**) MacDonald (2006). S_P = primary spine; S_S = secondary spine. (**1–7**) Scale bars = 50 μm; (**8–19**) scale bars = 100 μm.

which provides a basis for referring them to the *H. spongium* combination established by Noble and Webby (2009). *H. spongium* is readily distinguishable from other Ordovician haplotaeniatids (Pouille et al., 2014; Perera et al., 2020; Perera and Aitchison, 2022) owing to its very large pores (up to 30 μm) and the less-spongy nature of the labyrinthine meshwork.

As shown in Fig. 9.6, some areas of the outermost meshwork exhibit an irregularly porous character developed as a result of attaining a significant degree of two-dimensionality to the meshwork. The two-dimensional porous meshwork is more characteristic of the lower Silurian genus *Gyrosphaera* Noble and Maletz (2000), which is presumed to be closely related to *Haplotaeniatum* due to the mutual spiraliform layering (Noble and Maletz,

https://doi.org/10.1017/jpa.2023.13 Published online by Cambridge University Press

2000; Jones and Noble, 2006). Our observations corroborate these assumptions, and the *H. spongium* may represent an immediate ancestor of lower Silurian gyrosphaerid forms.

Family Inaniguttidae Nazarov and Ormiston, 1984, sensu Noble, 1994 and Danelian and Popov, 2003

Genus *Inanigutta* Nazarov and Ormiston, 1984, sensu Nazarov, 1988 and Perera and Aitchison, 2022

Type species.—*Entactinia unica* Nazarov, 1975 (GIN 4333/2) from the Bestamak Formation, southwest foothills of the Chingiz Range, eastern Kazakhstan by original designation.

Inanigutta complanata (Nazarov, 1975)
Figure 2.4

1975 *Entactinia complanata* Nazarov, p. 56, pl. 15, figs. 11, 12, pl. 20, figs 7, 8.
1980 *Entactinia complanata*; Nazarov and Popov, p. 29, pl. 1, figs. 2, 5, pl. 7, figs. 3, 4, pl. 11, figs. 3, 4, text-fig. 10.
1984 *Inanigutta complanata*; Nazarov and Ormiston, pl. 4, fig. 1.
?1992 *Inanigutta* cf. *I. complanata* Goto, Umeda, and Ishiga, p. 159, pl. 9, figs. 1–3.
1993 *Inanigutta complanata*; Wang, p. 99, pl. 10, figs. 1, 2.
2001 ?*Inanigutta complanata* Danelian and Floyd, p. 493, fig. 4a.
2009 *Inanigutta complanata*; Noble and Webby, pl. 5, figs. 10, 11, pl. 6, fig. 14.
?2020 *Inanigutta* sp. cf. *I. complanata*; Perera et al., p. 2040, pl. 1, fig. i.
2022 *Inanigutta complanata*; Perera and Aitchison, p. 16, fig. 11.9.

Holotype.—Specimen (GIN 4333/29) from the Middle Ordovician, Bestamak Formation, southwestern foothills of the Chingiz Range, eastern Kazakhstan (Nazarov, 1975, pl. 20, fig. 8).

Remarks.—Specimens encountered are identical to those described by Noble and Webby (2009). No further investigation was undertaken as this taxon has been extensively studied in all encounters since 1984.

Genus *Kalimnasphaera* Webby and Blom, 1986

Type species.—*Kalimnasphaera maculosa* Webby and Blom, 1986 (AM.F. 134783) from limestone breccias of the Malongulli Formation of New South Wales, Australia, by original designation.

Kalimnasphaera maculosa Webby and Blom, 1986
Figure 2.1

1976 Spumellaria; Dunham and Murphy, p. 884, pl. 1, figs. 1–5.
1986 *Kalimnasphaera maculosa* Webby and Blom, p. 152, figs. 3.4–3.9, 4.1–4.8.
1990 *Kalimnasphaera* sp. aff. *K. maculosa*; Renz, p. 370, pl. 2, figs. 6, 8–10.
1992 *Kalimnasphaera* sp. aff. *K. maculosa*; Goto, Umeda, and Ishiga, p. 159, pl. 8, figs. 1–3.
2009 *Kalimnasphaera maculosa*; Noble and Webby, p. 559, figs. 5.12–5.15, 6.13.

Holotype.—Specimen (AM.F. 134783)) from the Malongulli Formation, New South Wales, Australia (Webby and Blom, 1986, pl. 3, fig. 4).

Remarks.—*K. maculosa* is common in other Katian radiolarian assemblages from which its skeletal microstructure has been thoroughly investigated. Micro-CT observations of *K. pingliangensis* Perera and Aitchison (2022) provide further insight into microscale features of the genus. Since hundreds of specimens encountered in this study are visually identical to the previous reports, no further investigation was undertaken.

Acknowledgments

The research was financially supported by the Australian Research Council grant no. ARC DP 1501013325 (to J.C.A.). We thank landholders in the Cliefden Caves area on the Belubula River—P. Agostino (Malongulli), B. Crossing (Angullong), and A. Dunhill (Boonderoo)—for kindly facilitating access to sample locations. We also thank C. Evans at the Julius Kruttschnitt Mineral Research Centre, UQ, for conducting micro-CT measurements of the radiolarian specimens. We gratefully acknowledge the helpful advice from Wiradjuri Condobolin Corporation and CEO A. Coe regarding appropriate indigenous nomenclature for the new genus *Wiradjuri*. The authors thank *Journal of Paleontology* Associate Editor P. Noble and the two reviewers, T. Danelian and anonymous, for their constructive comments and guidance that helped to improve this manuscript. This paper is a contribution to the International Geoscience Programme (IGCP) Project 735: Rocks and the Rise of Ordovician Life.

Declaration of competing interests

The authors declare none.

Data availability statement

Data available from the Dryad Digital Repository: https://doi.org/10.5061/dryad.qfttdz0n9

References

Afanasieva, M.S., 2000, New radiolarians of the superfam-ily Entactinoidea from the Upper Devonian of Timan-Pechora Province, Russia: Paleontological Journal, v. 34, p. 131–146.
Aitchison, J.C., and Stratford, J.M.C., 1997, Middle Devonian (Givetian) Radiolaria from eastern New South Wales, Australia; a reassessment of the Hinde (1899) fauna: Neues Jahrbuch für Geologie und Paläontologie, Abhandlungen, v. 203, p. 369–390.
Aitchison, J.C., Suzuki, N., Caridroit, M., Danelian, T., and Noble, P., 2017a, Paleozoic radiolarian biostratigraphy, *in* Danelian, T., Caridroit, M., Noble, P., and Aitchison, J.C., eds., Catalogue of Paleozoic Radiolarian Genera: Geodiversitas, v. 39, p. 503–531.
Aitchison, J.C., Suzuki, N., and O'Dogherty, L., 2017b, Inventory of Paleozoic radiolarian species (1880–2016), *in* Danelian, T., Caridroit, M., Noble, P., and Aitchison, J.C., eds., Catalogue of Paleozoic Radiolarian Genera: Geodiversitas, v. 39, p. 533–637.

https://doi.org/10.1017/jpa.2023.13 Published online by Cambridge University Press

Cavalier-Smith, T., 1987, The origin of eukaryotic and archaebacterial cells: Annals of the New York Academy of Sciences, v. 503, p. 17–54.
Colquhoun, G.P., Hughes, K.S., Deyssing, L., Ballard, J.C., Folkes, C.B., Phillips, G., Troedson, A.L., and Fitzherbert, J.A., 2021, New South Wales Seamless Geology dataset, version 2.1: Maitland, Geological Survey of New South Wales, Department of Regional NSW.
Cooper, R.A., Maletz, J., Taylor, L., and Zalasiewicz, J.A., 2004, Graptolites: patterns of diversity across paleolatitudes, *in* Webby, B.D., Paris, F., Droser, M.L., and Percival, I.G., eds., The Great Ordovician Biodiversification Event: New York, Chichester, West Sussex: Columbia University Press, p. 281–293.
Danelian, T., and Floyd, J., 2001, Progress in describing Ordovician siliceous biodiversity from the Southern Uplands (Scotland, UK): Transactions of the Royal Society of Edinburgh, Earth Sciences, v. 91, p. 489–498.
Danelian, T., and Monnet, C., 2021, Early Paleozoic radiolarian plankton diversity and the Great Ordovician Biodiversification Event: Earth-Science Reviews, v. 218, n. 103672, https://doi.org/10.1016/j.earscirev.2021.103672.
Danelian, T., and Popov, L., 2003, Ordovician radiolarian biodiversity: insights based on new and revised data from Kazakhstan: Bulletin de la Société Géologique de France, v. 174, p. 325–335.
Deflandre, G., 1953, Radiolaires fossils, *in* Grassé, P.P., ed., Traité de Zoologie: Paris, Masson, p. 389–436. [in French]
Dumitrica, P., Caridroit, M., and De Wever, P., 2000, Archae-ospicularia, ordre nouveau de radiolaires: une nouvelle étape pour la classification des radiolaires du Paléozoïque inférieur: Comptes Rendus de l'Académie des Sciences Paris, Sciences de la Terre et des planets, v. 330, p. 563–569.
Dunham, J.B., and Murphy, M.A., 1976, An occurrence of well-preserved radiolarian from the Upper Ordovician (Caradocian), Eureka County, Nevada: Journal of Paleontology, v. 50, p. 882–887.
Ehrenberg, C.G., 1838, Über die bildung der kreidefelsen und des kreidemergels durch unsichtbare organismen: Abhandlungen der Königlichen Preussichen Akademie der Wissenschaften zu Berlin, v. 1838, p. 59–147. [in German]
Ehrenberg, C.G., 1876, Fortsetzung der mikrogeologischen Studienals Gesammt-Uebersicht der mikroskopischen Paläontologie gleichartig analysirter Gebirgsarten der Erde, mit specieller Rücksicht auf den Polycystinen-Mergel von Barbados: Abhandlungen der Königlichen Preussichen Akademie der Wissenschaften zu Berlin, v. 1876, 226 p. [in German]
Foreman, H.P., 1963, Upper Devonian Radiolaria from the Huron Member of the Ohio Shale: Micropaleontology, v. 9, p. 267–304.
Furutani, H., 1990, Middle Paleozoic radiolarians from Fukuji Area, Gifu Prefecture, central Japan: Journal of Earth Sciences Nagoya University, v. 37, p. 1–56.
Glen, R.A., Walshe, J.L., Barron, L.M., and Watkins, J.J., 1998, Ordovician convergent-margin volcanism and tectonism in the Lachlan sector of east Gondwana: Geology, v. 26, p. 751–754.
Glen, R.A., Quinn, C.D., and Cooke, D.R., 2012, The Macquarie Arc, Lachlan Orogen, New South Wales: its evolution, tectonic setting and mineral deposits: Episodes, v. 35, p. 177–186.
Goldman, D., Sadler, P.M., Leslie, S.A., Melchin, M.J., Agterberg, F.P., and Gradstein, F.M., 2020, The Ordovician Period, *in* Gradstein, F.M., Ogg, J.G., Schmitz, M.D., and Ogg, G.M., eds., Geologic Time Scale 2020: Amsterdam, Elsevier, p. 631–694.
Goodbody, Q.H., 1986, Wenlock Palaeoscenidiidae and Entactiniidae (Radiolaria) from the Cape Phillips Formation of the Canadian Arctic Archipelago: Micropaleontology, v. 32, p. 129–157.
Goto, H., and Ishiga, H., 1991, Study of Late Ordovician radiolarians from the Lachlan Fold Belt, southeastern Australia: Geology Research Report, Shimane University, v. 10, p. 57–62. [in Japanese with English abstract]
Goto, H., Umeda, M., and Ishiga, H., 1992, Late Ordovician radiolarians from the Lachlan Fold Belt, southeastern Australia: Memoirs of the Faculty of Science, Shimane University, v. 26, p. 145–170.
Holdsworth, B.K., 1969, Namurian Radiolaria of the genus *Ceratoikiscum* from Staffordshire and Derbyshire, England: Micropaleontology, v. 15, p. 221–229.
Holdsworth, B.K., 1977, Paleozoic Radiolaria: stratigraphic distribution in Atlantic borderlands, *in* Swain, F.M., ed., Stratigraphic Micropaleontology of Atlantic Basin and Borderlands: Amsterdam, Elsevier, p. 167–184.
Jablonski, D., 1991, Extinctions: a paleontological perspective: Science, v. 253, p. 754–757.
Jones, M.K., and Noble, P.J., 2006, Sheinwoodian (uppermost lower Silurian) Radiolaria from the Cape Phillips Formation, Nunavut, Canada: Micropaleontology, v. 52, p. 289–315.
Kachovich, S., and Aitchison, J.C., 2020, Micro-CT study of Middle Ordovician Spumellaria (radiolarians) from western Newfoundland, Canada: Journal of Paleontology, v. 94, p. 417–435.
Kachovich, S., Sheng, J., and Aitchison, J.C., 2019, Adding a new dimension to investigations of early radiolarian evolution: Scientific Reports, v. 9, n. 6450, https://doi.org/10.1038/s41598-019-42771-0.
Keble, R.A., and Harris, W.J., 1925, Graptolites from Mt. Eastern: Records of the Geological Survey of Victoria, v. 4, p. 507–516.
Kozur, H.W., and Mostler, H., 1982, Entactinaria subordo nov., a new radiolarian suborder: Geologisch Paläontologische Mitteilungen Innsbruck, v. 11, p. 399–414.
Li, H.S., 1995, New genera and species of Middle Ordovician Nassellaria and Albaillellaria from Baijingsi, Quilian Mountains, China: Scientia Geologica Sinica, v. 4, p. 331–346.
MacDonald, E.W., 1998, Llandovery Secuicollactinae and Rotasphaeridae (Radiolaria) from the Cape Phillips Formation, Cornwallis Island, Arctic Canada: Journal of Paleontology, v. 72, p. 585–604.
MacDonald, E.W., 1999, *Insolitignum* n.gen. and *Palaeoephippium* Goodbody 1986 (Radiolaria) from the lower Silurian of the Cape Phillips Formation, Arctic Canada: Canadian Journal of Earth Science, v. 36, p. 2051–2057.
MacDonald, E.W., 2003, *Radiolaria from the lower Silurian of the Cape Phillips Formation, Cornwallis Island, Nunavut, Canada* [Ph.D. thesis]: Halifax, Dalhousie University, 370 p.
MacDonald, E.W., 2004, Palaeoscenidiidae (Radiolaria) from the lower Silurian of the Cape Phillips Formation, Cornwallis Island, Nunavut, Canada: Journal of Paleontology, v. 78, p. 257–274.
MacDonald, E.W., 2006, Haplotaeniatumidae and Inaniguttidae (Radiolaria) from the lower Silurian of the Cape Phillips Formation, Cornwallis Island, Nunavut, Canada: Journal of Paleontology, v. 80, p. 19–37.
Maletz, J., and Bruton, D.L., 2008, The Middle Ordovician *Proventocitum procerulum* radiolarian assemblage of Spitsbergen and its biostratigraphic correlation: Palaeontology, v. 51, p. 1181–1200.
Moors, H.T., 1970, Ordovician graptolites from the Cliefden Caves area, Mandurama, NSW, with a reappraisal of their stratigraphic significance: Proceedings of the Royal Society of Victoria, v. 83, p. 253–288.
Nazarov, B.B., 1975, Lower and middle Paleozoic Radiolaria of Kazakhstan (methods of investigation, systematics and stratigraphy): Akademiya Nauk SSSR, Trudy Geologicheskogo Instituta, Akademiya Nauk SSSR, v. 275, 202 p. [in Russian]
Nazarov, B.B., 1988, Paleozoic Radiolaria. Practical Manual of Microfauna of the USSR, Volume 2: Leningrad, Nedra, 232 p. [in Russian]
Nazarov, B.B., and Ormiston, A., 1984, Tentative system of Paleozoic Radiolaria, *in* Petrushevskaya, M.G., and Stepanjants, S.D., eds., Morphology, Ecology and Evolution of Radiolarians: Material from the IV Symposium of European Radiolarists EURORAD IV, Academiya Nauk SSSR, Zoological Institute, Leningrad, USSR, p. 64–87. [in Russian with English summary]
Nazarov B.B., and Ormiston, A.R, 1987, A new Carboniferous radiolarian genus and its relation to the multishelled entactiniids: Micropaleontology, v. 33, p. 66–73.
Nazarov, B.B., and Ormiston, A.R., 1993, New biostratigraphically important Paleozoic Radiolaria of Eurasia and North America, *in* Blueford, J.R., and Murchey, B.L., eds., Radiolaria of Giant and Subgiant Fields in Asia: Nazarov Memorial Volume, Micropaleontology, Special Publication, v. 6. p. 22–60.
Nazarov, B.B., and Popov, L.Y., 1980, Stratigraphy and fauna of the siliceous carbonate sequence of the Ordovician of Kazakhstan (Radiolaria and inarticulate brachiopods): Transactions of the Geological Institute of the Soviet Academy of Sciences, v. 331, 192 p. [in Russian]
Noble, P.J., 1994, Silurian Radiolarian Zonation for the Cabal-los Novaculite, Marathon Uplift, West Texas: Bulletins of American Paleontology, v. 106, 55 p.
Noble, P.J., 2000, Revised stratigraphy and structural relationships in the Roberts Mountains allochthon of Nevada (USA) based on radiolarian cherts, *in* Cluer, J.K., Price, J.G., Struhsacker, E.M., Hardyman, R.F., and Morris, C.L., eds., Geology and Ore Deposits 2000: The Great Basin and Beyond: Symposium Proceedings: Reno, Geological Society of Nevada, p. 439–449.
Noble, P.J., and Maletz, J., 2000, Radiolaria from the Telychian (Llandovery, Early Silurian) of Dalarna, Sweden: Micropaleontology, v. 46, p. 265–275.
Noble, P.J., and Webby, B.D., 2009, Katian (Ordovician) radiolarians from the Malongulli Formation, New South Wales, Australia, a re-examination: Journal of Paleontology, v. 83, p. 548–561.
Noble, P.J., Braun, A., and McClellan, W., 1998, *Haplotaeniatum* faunas (Radiolaria) from the Llandoverian (Silurian) of Nevada and Germany: Neues Jahrbuch für Geologie und Paläontologie, Monatshefte, v. 12, p. 705–726.
Noble, P., Aitchison, J.C., Danelian, T., Dumitrica, P., Maletz, J., Suzuki, N., Cuvelier, J., Caridroit, M., and O'Dogherty, L., 2017, Taxonomy of Paleozoic radiolarian genera, *in* Danelian, T., Caridroit, M., Noble, P., and Aitchison, J.C., eds., Catalogue of Paleozoic Radiolarian Genera: Geodiversitas, v. 39. p. 419–502.
Obut, O.T., 2022, Early Paleozoic plankton evolution in the Paleo-Asian Ocean: insights from new and reviewed fossil records from the Gorny Altai, West Siberia: Paleontological Research, v. 27, p. 3–13.

Percival, I.G., 1976, The geology of the Licking Hole Creek area, near Walli, central western New South Wales: Journal and Proceedings of the Royal Society of New South Wales, v. 109, p. 7–23.
Percival, I.G., and Glen, R.A., 2007, Ordovician to earliest Silurian history of the Macquarie Arc, Lachlan Orogen, New South Wales: Australian Journal of Earth Sciences, v. 54, p. 143–165.
Percival, I.G., and Webby, B.D., 1996, Island benthic assemblages: with examples from the late Ordovician of Eastern Australia: Historical Biology, v. 11, p. 171–185.
Percival, I.G., Kraft, P., Zhang, Y., and Sherwin, L., 2015, A long-overdue systematic revision of Ordovician graptolite faunas from New South Wales, Australia: Stratigraphy, v. 12, p. 48–54.
Percival, I.G., Engelbretsen, M.J., Brock, G.A., and Farrell, J.R., 2016, Ordovician (Darriwilian–Katian) lingulate brachiopods from central New South Wales, Australia: Memoirs of the Association of Australasian Palaeontologists, v. 49, p. 447–484.
Perera, S., and Aitchison, J.C., 2022, Late Sandbian (Sa2) radiolarians of the Pingliang Formation from the Guanzhuang section, Gansu Province, China: Journal of Paleontology, v. 96, p. 19–45.
Perera, S., Aitchison, J.C., and Nothdurft, L., 2020, Middle Ordovician (Darriwilian) radiolarians from the Crawford Group, Scotland: Geological Magazine, v. 157, p. 2033–2043.
Pouille, L., Danelian, T., and Popov, L.E., 2014, A diverse upper Darriwilian radiolarian assemblage from the Shundy Formation of Kazakhstan: insights into late Middle Ordovician radiolarian biodiversity: Journal of Micropalaeontology, v. 33, p. 149–163.
Renz, G.W., 1990, Late Ordovician (Caradocian) radiolarians from Nevada: Micropaleontology, v. 36, p. 367–377.
Riedel, W.R., 1967, Some new families of Radiolaria: Proceedings of the Geological Society of London, v. 1640, p. 148–149.
Rigby, J.K., and Webby, B.D., 1988, Late Ordovician sponges from the Malongulli Formation of central New South Wales, Australia: Palaeontographica Americana, v. 56, p. 5–14.
Rüst, D., 1892, Beiträge zur Kenntnis der fossilen Radiolarien aus Gesteinen der Trias und der Palaeozoischen Schichten: Palaeontographica, v. 38, p. 107–192.
Sheehan, P.M., 2001, The Late Ordovician mass-extinction: Annual Review of Earth and Planetary Sciences, v. 29, p. 331–364.
Sheng, J., Kachovich, S., and Aitchison, J. C., 2020, Skeletal architecture of middle Cambrian spicular (archeoentactiniid) radiolarians revealed using micro-CT: Journal of Micropalaeontology, v. 39, p. 61–76.
Song, Q.Y., Cui, Z.L., Hua, H., and Wang, X.R., 2000, The Late Ordovician Radiolaria from Fuping of Shaanxi Province, China: Journal of Northwest University (Natural Science Edition), v. 30, p. 65–68. [in Chinese with English abstract]
Stait, B., Webby, B.D., and Percival, I.G., 1985, Late Ordovician nautiloids from central New South Wales, Australia: Alcheringa, v. 9, p. 143–157.
Stevens, N.C., 1952, Ordovician stratigraphy at Cliefden Caves, near Mandurama, New South Wales: Proceedings of the Linnean Society of New South Wales, v. 77, p. 114–120.
Tetard, M., Danelian, T., and Noble, P., 2014, Biostratigraphical and palaeobiogeographical implications of lower Silurian Radiolaria from black cherts of the Armorican Massif (France): Journal of Micropalaeontology, v. 33, p. 165–178.
Trotter, J.A., and Webby, B.D., 1994, Upper Ordovician conodonts from the Malongulli Formation, Cliefden Caves area, central New South Wales: AGSO Journal of Australian Geology and Geophysics, v. 15, p. 475–499.
Umeda, M., and Suzuki, Y., 2005, Aeronian (Llandovery, early Silurian) radiolarians from the Kallholn Formation in Siljan District, Sweden: Micropaleontology, v. 51, p. 83–91.
Wakamatsu, H., Sugiyama, K., and Furutani, H., 1990, Silurian and Devonian radiolarians from the Kurosegawa Tectonic Zone, southwest Japan: Journal of Earth Sciences, Nagoya University, v. 37, p. 157–192.
Wang, Y., 1993, Middle Ordovician radiolarians from the Pingliang Formation of Gansu Province, China, *in* Blueford, J.R., and Murchey, B.L., eds., Radiolaria of Giant and Subgiant Fields in Asia: Nazarov Memorial Volume, Micropaleontology Special Publication No. 6, p. 98–114.
Wang, Y., and Zhang, Y.D., 2011, Radiolarian fauna of the Wufeng Formation (Upper Ordovician) in Lunshan Area, Jiangsu and its geological significance: Acta Micropalaeontologica Sinica, v. 28, p. 251–260. [in Chinese with English summary]
Webby, B.D., 1992, Ordovician island biotas: New South Wales record and global implications: Journal and Proceedings of the Royal Society of New South Wales, v. 125, p. 51–77.
Webby, B.D., and Blom, W., 1986, The first well-preserved radiolarians from the Ordovician of Australia: Journal of Paleontology, v. 60, p. 145–157.
Webby, B.D., and Packham, G.H., 1982, Stratigraphy and regional setting of the Cliefden Caves Limestone Group (Late Ordovician), central-western New South Wales: Journal of the Geological Society of Australia, v. 29, 297–317.
Webby, B.D., and Trotter, J., 1993, Ordovician sponge spicules from New South Wales, Australia: Journal of Paleontology, v. 67, p. 28–41.
Won, M.Z., 1997, Review of family Entactiniidae (Radiolaria), and taxonomy and morphology of Entactiniidae in the Late Devonian (Frasnian) Gogo Formation, Australia: Micropaleontology, v. 43, p. 333–369.
Won, M.Z., Blodgett, R.B., and Nestor, V., 2002, Llandoverian (early Silurian) radiolarians from the Road River Formation of East-Central Alaska and the new family Haplotaeniatumidae: Journal of Paleontology, v. 76, p. 941–964.
Zhang, Z., Luo, H., and Zhang, Y.D., 2018, Radiolaria faunas of the Wufeng Formation (Upper Ordovician) at Lunshan, Jiangsu Province and Yihuang-1 Well, Yichang, Hubei Province, China: Acta Micropalaeontologica Sinica, v. 35, p. 170–180. [in Chinese with English abstract]
Zhen, Y-Y., and Webby, B.D., 1995, Upper Ordovician conodonts from the Cliefden Caves Limestone Group, central New South Wales, Australia: Courier Forschungsinstitut Senckenberg, v. 182, p. 265–305.

Accepted: 2 February 2023